SEISMIC RESPONSE OF SIMPLE NONLINEAR HYSTERETIC STRUCTURES

by

S. R. Malushte and M. P. Singh

Technical Report of Research Supported by
The National Science Foundation Under
Grant Numbers CEE-8214070 and CEE-8412830

Department of Engineering Science & Mechanics
Virginia Polytechnic Institute & State University
Blacksburg, Virginia 24061

April 1987

BIBLIOGRAPHIC DATA SHEET	1. Report No. VPI-E-87-4	2.	3. Recipient's Accession No. PB88-232376/AS

4. Title and Subtitle
Seismic Response of Simple Nonlinear Hysteretic Structures

5. Report Date
April 1987

6.

7. Author(s)
S. R. Malushte and M. P. Singh

8. Performing Organization Rept. No.

9. Performing Organization Name and Address
Virginia Polytechnic Institute & State University
Blacksburg, Virginia 24061

10. Project/Task/Work Unit No.

11. Contract/Grant No.
CEE-8214070 and
CEE-8412830

12. Sponsoring Organization Name and Address
National Science Foundation
Washington, D.C. 20550

13. Type of Report & Period Covered
Technical

14.

15. Supplementary Notes

16. Abstracts Seismic response of single-degree-of-freedom oscillators with elasto-plastic and bilinear hysteretic stiffness characteristics is studied using exact time history analysis and equivalent linear analysis performed with five non-hysteretic nonlinear models which are equivalent to a hysteretic model. To use the nonlinear models, the technique of the stochastic linearization is adopted with the assumption of a zero mean, stationary Gaussian response. The accuracy of the equivalent linearization results is checked by comparing them with the time history ensemble results obtained with the exact time history solution developed in this work. It is observed that the comparison is satisfactory for responses corresponding to low ductility ratios. For large inelastic deformations, the response is not zero mean and the equivalent linearization results obtained with equivalent nonlinear models are not satisfactory. In such a case a direct linearization of the hysteretic model is likely to improve results.

17. Key Words and Document Analysis. 17a. Descriptors

Earthquakes, Hysteretic Behavior, Structures, Nonlinear Analysis, Energy Dissipation, Oscillators, Spectra, Equivalent linear, Seismic Response, Dynamic Response, Vibration, Time history.

17b. Identifiers/Open-Ended Terms

17c. COSATI Field/Group

18. Availability Statement	19. Security Class (This Report)	21. No. of Pages
Unlimited Release	UNCLASSIFIED	102
	20. Security Class (This Page) UNCLASSIFIED	22. Price A06 19.95

Acknowledgements

This report is the thesis of Sanjeev R. Malushte which was submitted to Virginia Polytechnic Institute and State University in partial fulfillment of the requirements of the degree of Master of Science in Engineering Mechanics.

This work was partially supported by National Science Foundation through Grant Nos. CEE-8214070 and 841280. This financial support is gratefully acknowledged. The opinion, findings and conclusions or recommendations expressed in this report are those of the writers and these do not necessarily reflect the views of the National Science Foundation.

TABLE OF CONTENTS

Chapter I

INTRODUCTION

In structural engineering, it is customary to use response spectra for the design of structural members subjected to earthquake excitation. Response spectra are generated for a range of frequency and damping. Usually this range is such that it is common for most structural systems. Also, response spectra correspond to a certain intensity of seismic excitation, which is a characteristic of the geological properties of the place where the structure is to be located. For normal design purposes, the maximum displacement, force and other relevant response parameters corresponding to a given natural frequency and damping of a structure can be obtained using the appropriate response spectrum. The structure is then designed to endure the response characteristics obtained in the above fashion.

It must be noted that most of the structures respond inelastically during a seismic occurence. However, the response spectra are generally constructed based on the assumption that the oscillator behaves elastically. They do not account for the fact that much of the energy is dissipated by inelastic yielding and/or hysteresis during such response. Hence, the conventional response spectra generally underestimate the design displacement. This explains the fact that many times failure of important structural elements, such as columns and beams, occurs due to the lack of provision of sufficient ductility in them.

In light of the above observations, it is necessary to construct response spectra which accommodate various possible inelastic behaviors of structural elements. In this thesis, several methods capable of predicting the response of hysteretically behaving, single-degree-of-freedom oscillators are studied. In general, it is not possible to obtain the exact solution for the response due to nonlinear, hysteretic behavior. Time history analysis using Newmark's or Wilson's method is always possible, but this is computationally expensive, hence unsuitable for normal structural designs. The purpose of this work is to explore simple methods which can be effectively used to study the response of hysteretic structures.

Commonly, the so called inelastic spectra are generated for specified levels of ductility. They define the magnitude of yield displacement required to cause the response of a desired ductility ratio. This idea was introduced by Newmark and Hall (28). Several investigators have since worked in this field to predict the response due to various types of nonlinear and/or hysteretic behavior. Significant work has been contributed by Caughey (6,7,8,9), Iwan and Gates (12,16,17,18,19), Wen and Baber (2,3,44,45), among others (11,13,23,24,28,35,39,41). The inelastic spectra for other response quantities are of the same nature as in the elastic spectra. The famous tripartite grid representation of the response characteristics can be done for inelastic oscillators, too(28,36).

It is common to use artificially generated earthquake time-histories of ground motion due to the scarcity of the records of authentic seismic ground motions. Typically, such records are based on the Kanai-Tajimi formulation. In this, the seismic input is assumed to be of white noise type (containing all possible frequencies). Depending on the properties of the underlying soil medium, the ground response spectra are represented as a wide or narrow band input of appropriate spectral density function. Various ensembles of artificially generated ground response spectra (earthquake time histories) were used for this thesis. The basis for such approach along with the characteristics of these ensembles is presented in chapter 4.

For random inputs, it is believed that acceptable solutions can be obtained by replacing the hysteretic character of the original system by an equivalent non-hysteretic but nonlinear system. This is done by defining suitable stiffness and damping parameters of non-hysteretic yet nonlinear nature. This eliminates the response dependance on its own time-history, a characteristic of hysteretic behavior. This idea was first introduced by Jacobsen(20) in his geometric energy approach. Since then, several such models have been proposed and studied, each using certain criteria to define the properties of the resulting non-hysteretic model (4,9,12,17,22,24,29,37,39). Typically, the names of these methods suggest the criteria used for their formulation. In this thesis, some such non-hysteretic models were studied. Five of these are presented in chapter 2. Equivalent linear properties of these non-hysteretic models were obtained using stochastic equivalent linearization approach, based on a mean square error minimization technique. The response of the original hysteretic oscillator is then approximated as the one caused in the equivalent linear oscillator. In this thesis, it is intended to examine these methods from accuracy and expense point of view. Also, the domains of natural frequency and ductility in which such methods can work satisfactorily are explored.

Exact closed form solutions were developed for elasto-plastic and bilinear, hysteretic systems. The results of such solutions were validated by a program based on Newmark's method (27) with very small time-step. All this formulation is presented in chapter 3. A computer program which implements the exact solutions was also developed. Inelastic response spectra and some other sample results were generated using this program. These results were also used for checking the accuracy of equivalent linear analysis approach, which is computationally inexpensive.

Chapter 4 deals with presentation of results based on the formulations developed in the preceding chapters. Some concluding remarks are also presented in this chapter.

Chapter II

METHODS USING EQUIVALENT LINEARIZATION APPROACH

2.1 INTRODUCTION

As mentioned in chapter 1, time-history analysis is computationally expensive. Thus it is necessary to develop simple, yet reasonably accurate methods for the prediction of seismic response of hysteretic structures. From a design point of view, it is important to note that we are interested only in the response statistics (mean, standard deviation, maxima, root mean square, etc). Whereas the time-history analysis produces an elaborate response history of the structure, the equivalent linearization approach leads to the computation of the vital characteristics such as those mentioned above. This justifies the use of simple yet effective methods like the ones presented in this chapter.

Exact solution is possible in very few cases of hysteretic behavior. In any case, such exact solutions result in expensive time-history analysis. Nonlinear differential equations of motion can be handled with the use of perturbation methods (11), equivalent linearization schemes, etc. It has been found that perturbation approach is not satisfactory for highly inelastic behavior. Some researchers have also attempted to use the Markovian process to model the hysteretic response (7); indeed, such response is a function of the previous response history. Equivalent linearization approach is a well accepted method in this regard and it is widely being used (2,3,8,12,14,16,17,23,24,39,41,45,46). In this chapter, a simple algorithm is developed for equivalent linearization of nonlinear, non-hysteretic systems. As mentioned in chapter 1, hysteretic structures can be modelled by equivalent non-hysteretic structures. In this chapter, some of these equivalent non-hysteretic models are presented. The equivalent linearization scheme used in this thesis is an indirect one, since it is carried out on the ensuing non-hysteretic model as opposed to carrying it out on the original hysteretic oscillator.

2.2 SYSTEMS CONSIDERED

Figure 1 shows a single-degree-of-freedom oscillator subjected to base excitation. The response characteristics of this oscillator depend on the stiffness and damping properties associated with the system as well as the nature and intensity of base excitation. The damping is caused due to viscous effects for ordinary structures under consideration. Such damping is directly proportional to the velocity of the oscillator at any instant and the viscous damping force acts in the direction opposite to the direction of motion.

For the systems considered in this work, the nonlinearity in the response is due to the hysteretic character of the force-displacement relationship. Figure 2 represents a perfectly elastic, non-hysteretic system. Figure 3 depicts an elasto-plastic, hysteretic behavior. A bilinear hysteretic system is represented in figure 4. An elasto-plastic behavior is a special case of the bilinear one in that the bilinear system has a non-zero stiffness along paths 2 and 4, unlike in the elasto-plastic systems. In both these cases, the response is characterized by paths 2 or 4 as long as the velocity does not become zero. The moment the velocity becomes zero, the system then behaves according to the nature characterized by path 3. Looking at figures 3 and 4, it is easy to see when the system changes its behavior from one path to another. Figure 5 portrays a general type of smooth hysteretic behavior. The velocity and/or response history dependance of the behavior of such systems may not be as simple and explicit as that in the elasto-plastic and bilinear hysteretic systems. These types of systems were not considered in this work. Their behavior may be modelled analytically by equations proposed by Wen, Bouc and Baber (2,3,5,45,46). It should be noted that all the systems considered in this work are of non-deteriorating type. The basic notation used is clearly indicated in above mentioned diagrams.

2.3 PROPOSED EQUIVALENT LINEARIZATION SCHEME

Consider the following type of equation of motion; applicable to nonlinear, non-hysteretic systems

$$m\ddot{x} + c_p(x)\ddot{x} + k_p(x)x = -ma(t) \tag{2.1}$$

We propose an equivalent linear system described by the following equation of motion

$$m\ddot{x} + c_e\dot{x} + k_e x = -\,ma(t) \tag{2.2}$$

where, C_e and K_e are the proposed equivalent linear properties of the given nonlinear system described by equation (2.1). Such approximate representation of the actual system introduces the following error, obtained as the difference between equations (2.1) and (2.2)

$$\varepsilon = [c_p(x) - c_e]\dot{x} + [k_p(x) - K_e]x \tag{2.3}$$

It has been shown that the mean square error minimization technique is at least as good as any other type (15). Hence, let us minimize the mean square error by defining C_e and K_e as follows

$$\frac{\partial}{\partial c_e}[E(\varepsilon^2)] = 0 \tag{2.4}$$

and

$$\frac{\partial}{\partial k_e}[E(\varepsilon^2)] = 0 \tag{2.5}$$

Equations (2.4) and (2.5) can be rewritten as

$$E[2\varepsilon \frac{\partial \varepsilon}{\partial c_e}] = 0 \tag{2.6}$$

and

$$E[2\varepsilon \frac{\partial \varepsilon}{\partial k_e}] = 0 \tag{2.7}$$

Substituting equation (2.3) in (2.6), we get

$$E[\{c_p(x) - C_e)\dot{x} + (k_p(x) - K_e)x\}(-\dot{x})] = 0 \tag{2.8}$$

or

$$E[c_p(x)\dot{x}^2] - C_e E[\dot{x}^2] + E[(k_p(x) - K_e)x\,\dot{x}] = 0 \tag{2.9}$$

If we assume that the response is stationary and Gaussian, then

$$E[(k_p(x) - k_e)x\,\dot{x}] = 0 \tag{2.10}$$

Hence, equation (2.9) can be rewritten as

$$C_e = \frac{E[c_p(x)\dot{x}^2]}{E[\dot{x}^2]} \tag{2.11}$$

But

$$E[c_p(x)\dot{x}^2] = E[c_p(x)]E[\dot{x}^2] \tag{2.12}$$

Substituting equation (2.12) in (2.11), we get

$$C_e = E[c_p(x)] \tag{2.13}$$

Now, substituting equation (2.3) in (2.7), we can write

$$E[\{(c_p(x) - C_e)\dot{x} + (k_p(x) - K_e)x\}] = 0 \tag{2.14}$$

or

$$E[(c_p(x) - C_e)x\,\dot{x}] - E[k_p(x)x^2] + K_e E[x^2] = 0 \tag{2.15}$$

Similar to equation (2.10), we have

$$E[(c_p(x) - C_e)x\,\dot{x}] = 0 \tag{2.16}$$

Substituting equation (2.16) in (2.15), we get

$$k_e = \frac{E[k_p(x)x^2]}{E[x^2]} \tag{2.17}$$

Equations (2.13) and (2.17) together define an equivalent linear system for the type of nonlinear systems described by equation (2.1).

We can further specialize equations (2.13) and (2.17) for a zero-mean, stationary, Gaussian response. The probability density function for such a distribution is given by

$$f_x(x) = \frac{1}{\sqrt{2\pi}\,\sigma_x} \mathrm{EXP}\left(-x^2/2\sigma_x^2\right) \tag{2.18}$$

Note that in this case, the mean value of 'x' is zero; this leads to the following result

$$E\left[x^2\right] = \sigma_x^2 \tag{2.19}$$

Now,

$$C_e = \int_{-\infty}^{\infty} c_p(x) f_x(x) dx \tag{2.20}$$

and

$$K_e = \frac{1}{\sigma_x^2} \int_{-\infty}^{\infty} x^2 k_p(x) f_x(x) dx \tag{2.21}$$

Substitution of equations (2.18) and (2.19) in (2.13) and (2.17) leads to the following results

$$C_e = \frac{1}{\sqrt{2\pi}\,\sigma_x} \int_{-\infty}^{\infty} c_p(x)\ \mathrm{EXP}\ \left(-x^2/2\sigma_x^2\right) dx \tag{2.22}$$

and

$$K_e = \frac{1}{\sqrt{2\pi}\,\sigma_x^3} \int_{-\infty}^{\infty} x^2 k_p(x)\ \mathrm{EXP}\ \left(-x^2/2\sigma_x^2\right) dx \tag{2.23}$$

Equations (2.22) and (2.23) define the equivalent damping and stiffness for a nonlinear, non-hysteretic system described by (differential) equation (2.1). It must be noted that these equations are valid only after we assume that the response is of stationary, Gaussian nature with zero mean.

It can be easily seen that the integrations in the (2.22) and (2.23) may not possess closed form solutions; yet they can be dealt with using Hermite's quadrature. In fact, in this work, Hermite's quadrature scheme for numerical integration was exclusively used to evaluate the equivalent linear properties. Let us define two functions g(x) and h(x) as below

$$g(x) = x^2 \, k_p(x) \tag{2.24}$$

and

$$h(x) = c_p(x) \tag{2.25}$$

Then using Hermite's quadrature for numerical integration, we can write

$$K_e \approx \frac{1}{\sqrt{\pi}} \sum_{i=1}^{n} g(\sqrt{2}\,\sigma_x\, x_i) W(x_i) \tag{2.26}$$

and

$$C_e \approx \frac{1}{\sqrt{\pi}} \sum_{i=1}^{n} h(\sqrt{2}\,\sigma_x\, x_i) W(x_i) \tag{2.27}$$

where, x_i = i^{th} root of the n^{th} order Hermite polynomial, $W(x_i)$= Weight corresponding to the above root Finally, ω_e, the equivalent natural frequency and β_e, the equivalent damping ratio are given as

$$\omega_e = \frac{2\pi}{T_e} = \omega_0 \sqrt{\frac{K_e}{k_0}} \tag{2.28}$$

and

$$\beta_e = \frac{C_e}{2\omega_e m} = C_E\left(\frac{T_e}{4\pi m}\right) \tag{2.29}$$

Where, T_e is the period of the equivalent linear system corresponding to an original hysteretic system with mass m, stiffness k_o, and natural frequency ω_o.

The systems considered for this work are of hysteretic nature, wherein the force-displacement characteristics are velocity dependent. In order that the above formulation be applicable to systems under consideration, it is necessary to define their equivalent nonlinear systems. Many such equivalent non-hysteretic models have been proposed and each one of them uses one or more criteria to define the equivalent non-hysteretic system. For the purpose of this thesis, five of these models were considered satisfactory and they are presented in the following paragraphs. In each case, the model is specialized for bilinear systems (elasto-plastic systems happen to be a special case of the bilinear ones with α=0).

Iwan and Gates (12,17) have extensively studied various non-hysteretic models and they arrived at many useful expressions for the application of those models. However, for the purpose of this work, it was aimed to model the stiffness and damping coefficient of hysteretic systems by using equivalent non-hysteretic models, hence, the expressions derived here are somewhat different than the ones obtained by Iwan and Gates. In all these models, it may be noted that the response is assumed to be of harmonic nature corresponding to any amplitude level under consideration.

2.4 HARMONIC EQUIVALENT LINEARIZATION (HEL)

In this method, an equivalent non-hysteretic system is obtained by characterizing the response to be of harmonic nature. This method has been studied by Caughey, Iwan, Gates (9,12,17). Following is a brief derivation of the results involved in this approach.

Harmonic response can be expressed as

$$x = A\cos(\omega t - \phi) = A\cos\theta \tag{2.30}$$

where, A=amplitude of the oscillations and ω=the frequency of the forcing function. The equation of motion for the given hysteretic oscillator is given by

$$\ddot{x} + 2\beta_0\omega_0\dot{x} + \omega_0^2 f(x,\dot{x}) = -a(t) \tag{2.31}$$

where, the function $f(x,\dot{x})$ symbolically represents the response dependance on its own response history. The equation of motion for the equivalent non-hysteretic oscillator can be written as

$$\ddot{x} + 2\beta_p(x)\omega_p(x)\dot{x} + \omega_p^2(x)x = -a(t) \tag{2.32}$$

The error involved in the above approximation is given by the difference between equations (2.32) and (2.31)

$$\delta(x) = 2\beta_0\omega_0\dot{x} + \omega_0^2 f(x,\dot{x}) - 2\beta_p(x)\omega_p(x)\dot{x} - \omega^2 p(x)x \qquad (2.33)$$

Let us define following variables

$$\xi_0 = 2\beta_0\omega_0 \text{ and } \xi_p(x) = 2\beta_p(x)\omega_p(x) \qquad (2.34)$$

Again, we stipulate that the best results are achieved using the mean square error minimization technique. Thus, following two conditions lead to the optimal equivalent parameters

$$\frac{\partial}{\partial \xi p}(\bar{\delta}^2) = 0 \qquad (2.35)$$

and

$$\frac{\partial}{\partial(\omega_p^2)}(\bar{\delta}^2) = 0 \qquad (2.36)$$

where $\bar{\delta}^2$ is the mean square error averaged over one oscillation of amplitude A

$$\bar{\delta}^2 = \frac{1}{T}\int_0^T \delta^2 dt \qquad (2.37)$$

Substituting equations (2.32) and (2.33) in (2.37), we get

$$\bar{\delta}^2 = \frac{1}{2\pi/\omega}\int_0^{2\pi/\omega} [\dot{x}(\xi_0 - \xi_p(A)) + \omega_0^2 f(x,\dot{x}) - \omega_p^2(A)x]^2 dt \qquad (2.38)$$

Now, equation (2.30) implies

$$\dot{x} = - A\omega\sin(\omega t - \phi) = - A\omega\sin\theta$$

and (2.39)

$$t = \frac{\theta + \phi}{\omega}$$

Hence,

$$f(x,\dot{x}) \equiv f(A\cos\theta, - A\omega\sin\theta)$$

and (2.40)

$$dt = \frac{d\theta}{\omega}$$

Substitution of (2.39) in (2.38) leads to the following expression

$$\bar{\delta}^2 = \frac{1}{2\pi} \int_0^{2\pi} [(\xi_o - \xi_p(A))(-A\omega\sin\theta) + \omega_o^2 f(A\cos\theta, - A\omega\sin\theta)\omega_p^2(A)A\cos\theta]^2 d\theta \tag{2.41}$$

Note that the equivalent non-hysteretic properties are a function of the amplitude of the oscillation only. Substituting (2.40) in (2.35), we get

$$0 = \frac{1}{2\pi} \int_0^{2\pi} 2[(-A\omega\sin\theta)(\xi_o - \xi_p(A)) + \omega_o^2 f(A\cos\theta, - A\omega\sin\theta) - \omega_p^2(A)A\cos\theta](-A\cos\theta)d\theta \tag{2.42}$$

Simplifying above expression, we get

$$\frac{1}{\pi} A^2\omega_p^2(A) \int_0^{2\pi} \cos^2\theta d\theta = \omega_o^2 A \frac{1}{\pi} \int_0^{2\pi} f(A\cos\theta, - A\omega\sin\theta)\cos\theta d\theta \tag{2.43}$$

or

$$\omega_p^2(A) = (\frac{\omega_o^2}{A})C(A) \tag{2.44}$$

where,

$$C(A) = \frac{1}{\pi} \int_0^{2\pi} f(A\cos\theta, - A\omega\sin\theta)\cos\theta d\theta \tag{2.45}$$

Also, substituting (2.40) in (2.36), we get

$$0 = \frac{1}{\pi}\int^{2\pi}[(-A\omega\sin\theta)(\xi_0 - \xi_p(A)) + \omega_0^2 f(A\cos\theta, -A\omega\sin\theta)$$
$$- \omega_p^2(A)A\cos\theta](-A\omega\sin\theta)d\theta \tag{2.46}$$

or

$$0 = \frac{1}{\pi}A^2\omega^2(\xi_p(A) - \xi_0)\int_0^{2\pi}\sin^2\theta d\theta + \omega_0^2 A\omega\frac{1}{\pi}\int_0^{2\pi}f(A\cos\theta, -A\omega\sin\theta)\sin\theta d\theta \tag{2.47}$$

Let us define

$$S(A) = \frac{1}{\pi}f(A\cos\theta, -A\omega\sin\theta)\sin\theta d\theta \tag{2.48}$$

then,

$$\xi_p(A) = \xi_0 - (\frac{\omega_0^2}{\omega_p})\frac{S(A)}{A} \tag{2.49}$$

or

$$\beta_p(A) = \beta_0(\frac{\omega_0}{\omega_p}) - \frac{1}{2}(\frac{\omega_0^2}{\omega_p^2})\frac{S(A)}{A} \tag{2.50}$$

Equation (2.49) is obtained after assuming resonant conditions on the equivalent non-hysteretic oscillator ($\omega=\omega_p$). Equations (2.43), (2.44), (2.47) and (2.49) define the (nonlinear) equivalent non-hysteretic properties of the original system. In terms of the damping coefficient, equation (2.50) may be written as (after multiplying by m)

$$c_p = c_0 - \frac{k_0}{\omega_p}\cdot\frac{S(A)}{A} \tag{2.51}$$

Now, let us specialize the above results for a bilinear, hysteretic system. Note that for an amplitude level less than the yield displacement, x_c, we have a linear, non-hysteretic response. Hence,

$$\omega_p^2(A) = \omega_0^2 \qquad (2.52a)$$

and $\qquad x_c < A < x_c$

$$\xi_p(A) = \xi_0 \qquad (2.52b)$$

Consider the case when $|A| > x_c$. Referring to figure 5, we can write

$$|A| = \mu x_c \qquad (2.53)$$

Now,

$$F(x,\dot{x}) = m\omega_0^2 f(A\cos\theta, - A\omega\sin\theta) = k_0 f(A\cos\theta, - A\omega\sin\theta) \qquad (2.54)$$

where, $F(x,\dot{x})$ = the restoring force in the spring. Again, referring to figure 5, we can write

$$\begin{aligned} f(x,\dot{x}) &= k_0 x_c + \alpha k_0 (x - x_c) \\ &= k_0(1 - \alpha)x_c + \alpha k_0 \left(\frac{A}{x_c}\right) x_c \cos\theta \qquad (2.55) \\ &= k_0 x_c[(1 - \alpha) = \alpha\mu\cos\theta] \end{aligned}$$

Comparing equations (2.52) and (2.53), we get

$$f(A\cos\theta, - A\omega\sin\theta) = x_c[\alpha\mu\cos\theta + (1 - \alpha)] \quad \text{along path 1} \quad (2.56a)$$

Likewise,

$$f(A\cos\theta, - A\omega\sin\theta) = x_c[\mu\cos\theta - (1 - \alpha)(\mu - 1)] \quad \text{along path 2} \quad (2.56b)$$

$$f(A\cos\theta, - A\omega\sin\theta) = x_c[\alpha\mu\cos\theta - (1 - \alpha)] \quad \text{along path 3} \quad (2.56c)$$

$$f(A\cos\theta, - A\omega\sin\theta) = x_c[\mu\cos\theta + (1 - \alpha)(\mu - 1)] \quad \text{along path 4} \quad (2.56d)$$

Referring to figure 4, we note that

$$(-A + 2x_c) < x < A \text{ and } \dot{x} > 0 \qquad (2.57)$$

In terms of μ, the ductility ratio and θ, the argument, we can express the above result as

$$-(\mu - 2) < \mu\cos\theta < \mu \qquad (2.58)$$

This may also be expressed as

$$(\pi + \theta^*) \geq \theta \geq 2\pi \qquad \text{along path 1} \quad (2.58a)$$

Likewise,

$$\theta^* \geq \theta \geq 0 \qquad \text{along path 2} \quad (2.58b)$$

$$\pi \geq \theta \geq \theta^* \qquad \text{along path 3} \quad (2.58c)$$

$$(\pi + \theta^*) \geq \theta \geq \pi \qquad \text{along path 4} \quad (2.58d)$$

where,

$$\theta^* = \cos^{-1}\left(\frac{\mu-2}{\mu}\right) \qquad (2.59)$$

Using equations (2.58) and (2.59), we can write

$$C(A) = \left(\frac{x_c}{2\pi}\right) \left\{ \int_0^{\theta^*} [\mu\cos\theta - (1-\alpha)(\mu-1)]\cos\theta d\theta + \int_\theta^\pi [\alpha\mu\cos\theta - (1-\alpha)]\cos\theta d\theta \right. \qquad (2.60)$$

$$\left. + \int_\pi^{\pi+\theta^*} [\mu\cos\theta + (1-\alpha)(\mu-1)]\cos\theta d\theta + \int_{\pi+\theta^*}^{2\pi} [\alpha\mu\cos\theta + (1-\alpha)]\cos\theta d\theta \right\}$$

and

$$S(A) = \left(\frac{x_c}{2\pi}\right)\left\{ \int_0^{\theta^*} [\mu\cos\theta - (1-\alpha)(\mu-1)]\sin\theta d\theta + \int_{\theta^*}^{\pi} [\alpha\mu\cos\theta - (1-\alpha)]\sin\theta d\theta \right. \tag{2.61}$$

$$\left. + \int_{\pi}^{\pi+\theta^*} [\mu\cos\theta + (1-\alpha)(\mu-1)]\sin\theta d\theta + \int_{\pi+\theta^*}^{2\pi} [\alpha\mu\cos\theta + (1-\alpha)]\sin\theta d\theta \right\}$$

Simplifying (2.60) and (2.61), we get

$$C(A) = \frac{\mu x_c}{\pi} \left[(1-\alpha) + \left(\theta^* - \frac{\sin 2\theta^*}{2}\right) + \alpha\pi\right] \tag{2.62}$$

and

$$S(A) = -\frac{\mu x_c}{\pi} (1-\alpha)\sin^2\theta^* \tag{2.63}$$

Substitute (2.53) and (2.63) in (2.62) and then substitute the resulting expression in (2.44) and (2.51). We thus get

$$\omega_p^2(\mu) = \frac{\omega_0^2}{\pi} \left\{(1-\alpha)\left(\theta^* - \frac{\sin 2\theta^*}{2}\right) + \alpha\pi\right\} \tag{2.64}$$

and

$$\beta_p(\mu) = \beta_0\left\{\alpha + \frac{(1-\alpha)}{\pi}\left(\theta^* - \frac{\sin 2\theta^*}{2}\right)\right\}^{-1/2} + \frac{1}{2}\left\{\alpha + \frac{(1-\alpha)}{\pi}\left(\theta^* - \frac{\sin 2\theta^*}{2}\right)\right\}\left\{\frac{(1-\alpha)\sin^2\theta^*}{\pi}\right\} \tag{2.65}$$

Using equation (2.53), we can write

$$\cos\theta^* = \left(\frac{\mu - 2}{\mu}\right), \quad \sin^2\theta^* = \frac{4}{\mu^2}(\mu - 1) \tag{2.66a}$$

and

$$\frac{\sin 2\theta^*}{2} = \frac{2}{\mu^2}(\mu - 2)\sqrt{\mu - 1} \tag{2.66b}$$

Substituting (2.66) in (2.64) and (2.65), we get

$$\omega_p(\mu) = \omega_o\{\alpha + \frac{(1-\alpha)}{\pi}[\cos^{-1}(\frac{\mu-2}{\mu}) - \frac{2}{\mu^2}(\mu-2)\sqrt{\mu-1}]\}^{1/2} \quad (2.67)$$

and

$$\beta_p(\mu) = \beta_o\{\frac{\omega_o}{\omega_p(\mu)}\}^{1/2} + \frac{2}{\pi}(1-\alpha)\frac{(\mu-1)}{\mu^2}\{\frac{\omega_o}{\omega_p(\mu)}\} \quad (2.68)$$

finally, in terms of the damping coefficient, we can write

$$c_p = c_o + (m\omega_o)\{\alpha + \frac{(1-\alpha)}{\pi}[\cos^{-1}(\frac{\mu-2}{\mu}) - \frac{2}{\mu^2}(\mu-2)\sqrt{\mu-1}]\}^{1/2}$$

$$x\{\frac{4(1-\alpha)}{\pi\mu^2}(\mu-1)\} \quad (2.69)$$

Equation (2.69) is obtained after substituting (2.67) into (2.46).

2.5 CONSTANT CRITICAL DAMPING (CCD)

This model was proposed by Jennings (22). In this method, the critical damping of the substitute non-hysteretic system is made equal to that of the given hysteretic system. This is accomplished as follows

$$k_p m_p = k_o m_o \quad (2.70)$$

or

$$\omega_p^2 m_p^2 = \omega_o^2 m_o^2 \quad (2.71)$$

Where, m_p, is the effective mass of the non-hysteretic model and m is the mass of the original hysteretic oscillator. The effective period for this method is defined the same as in the HEL method. The effective damping is found by equating the resonant amplitudes and dissipated energies of the given yielding system and the non-hysteretic system. This is done as below

$$\Delta W_p(A) = \Delta W(A) \tag{2.72}$$

where, $\Delta W_p(A)$=energy dissipated by the equivalent non-hysteretic system per a cycle of oscillation of amplitude A and $\Delta W(A)$= energy dissipated per a cycle of oscillation of the given yielding system

$$\Delta W_p(A) = \int_0^T (c\dot{x})\dot{x}dt \tag{2.73}$$

Let us substitute the following relationships

$$T = \frac{2\pi}{\omega_p} \tag{2.74}$$

and

$$\dot{x} = - A\omega\sin\omega t \tag{2.75}$$

Using above equations, we get

$$\Delta W_p(A) = \int_0^{2\pi/\omega} c_p\omega^2A^2\sin^2\omega t dt$$

$$= c_p\omega A^2\pi \tag{2.76}$$

Equation (2.76) is obtained after substituting $\omega=\omega_p$ at resonance. Also,

$$\Delta W(A) = H(A) + V(A) \tag{2.77}$$

where, H(A)=Area of the hysteresis loop ABCD shown in figure 4 and V(A)=Viscous energy dissipated by the yielding system. From fig 4, it can be seen that for a bilinear system

$$H(A) = 4k_0x_c^2(1 - \alpha)(\mu - 1) \tag{2.78}$$

Also,

$$V(A) = c_o \omega_p x_m^2 \pi \tag{2.79}$$

substituting above two equations in (2.77), we get

$$c_p \omega_p x_m^2 \pi = c_o \omega_p x_m^2 \pi + 4k_o x_c^2 (1 - \alpha)(\mu - 1) \tag{2.80}$$

Solving for c_p, we can write

$$c_p = c_o + \frac{4(1 - \alpha)}{\pi \mu^2} \left(\frac{k_o}{\omega_p}\right)(\mu - 1) \tag{2.81}$$

Substituting (2.67) in (2.81), we get

$$c_p = \left\{\alpha + \frac{(1 - \alpha)}{\pi} \left[\cos^{-1} \left(\frac{\mu - 2}{\mu}\right) - \frac{2}{\mu^2} (\mu - 2) \sqrt{\mu - 1} \right]\right\}^{-1/2} \tag{2.82}$$

Equations (2.67) and (2.82) together define the equivalent non-hysteretic system for given properties of a bilinear hysteretic system.

It is important to note that for this method, the equation (2.29) is modified as below

$$\beta_e \Big|_{CCD} = \frac{C_e}{2\omega_o m} \tag{2.83}$$

The reason for the above variation is explained in brief by the following formulation

$$\omega_e m_e = E(\omega_p m_p)$$

$$= E\left[\sqrt{\frac{k_p}{m_p}}\, m_p \right]$$

$$= \sqrt{k_o \omega_o} \tag{2.84}$$

$$\omega_e m_e = m\omega_o$$

2.6 GEOMETRIC STIFFNESS (GS)

This model was introduced by Berg (4) and Rosenblueth (37). In this method, the effective stiffness is specified by using the geometry of the hysteresis loop of the yielding system. The concept of secant stiffness is often used in this context. In reference to a bilinear system, we can write

$$k_p(A) = \frac{L(BE)}{L(OE)}$$

$$= \frac{k_o x_c + \alpha k_o (A - x_c)}{A} \tag{2.85}$$

or

$$k_p(\mu) = k_o\left[\alpha + \frac{1 - \alpha}{\mu}\right] \; ; \; \mu > 1 \tag{2.86}$$

Hence, the effective frequency is written as

$$\frac{\omega_p}{\omega_o} = \left[\frac{k_p}{k_o}\right]^{1/2}$$

$$= \left[\alpha + \frac{(1 - \alpha)}{\mu}\right]^{1/2} \tag{2.87}$$

Again, the effective damping is found by equating the resonant amplitudes and energies dissipated in the two systems. Hence, the effective damping is given by equation (2.81). Substituting (2.87) in (2.81), we get

$$c_p = c_0 + \left[\alpha + \frac{(1 - \alpha)}{\mu}\right]^{-1/2} \left\{\frac{4(1 - \alpha)}{\pi} (m\omega_0)\left(\frac{\mu - 1}{\mu^2}\right)\right\} \qquad (2.88)$$

Equations (2.87) and (2.88) together define the properties of the substitute non-hysteretic system. This method was used by Singh and Ashtiany (39,40) to model Ramberg-Osgood type of nonlinear behavior (34).

The following two methods use the results of the geometric stiffness method to find average system properties corresponding to an amplitude of A.

2.7 AVERAGE STIFFNESS & DAMPING (ASD)

This idea behind this method was proposed by Newmark and Rosenbleuth (29). In this work, however, the averaged quantities are stiffness and damping coefficient, unlike in their method, where period and damping ratio are the averaged quantities (Average Period & Damping). These can be applied to any nondeteriorating SDOF system under a condition that the system has equal yield for positive and negative displacements. As the name suggests, the stiffness and damping of the effective non-hysteretic system is obtained by averaging the expressions for the same quantities as developed in the geometric stiffness scheme. This is done as below

$$k_p(A) = \frac{1}{A} \int_0^A k_p(a)da \qquad (2.89)$$

and

$$c_p(A) = \frac{1}{A} \int_0^A c_p(a)da \qquad (2.90)$$

Specializing for a bilinear system, we get

$$k_p(A) = \frac{1}{a}\left[\int_0^{x_c} k_o da + \int_{x_c}^{A} k_o[\alpha + \frac{1-\alpha}{\mu_a}] da\right] \tag{2.91}$$

But

$$\mu_a = \frac{a}{x_c} \therefore da = x_c \, d\mu_a \tag{2.92}$$

Carrying out the integration, we get

$$k_p(\mu) = \frac{k_o}{\mu}\{1 + \alpha(\mu - 1) + (1 - \alpha)\ln\mu\} \;;\; \mu > 1 \tag{2.93}$$

Let us make the following substitution in equation (2.90)

$$x = x_c\lambda, \quad dx = x_c d\lambda \tag{2.94}$$

Substituting above relations, we get

$$c_p(\mu) = \frac{1}{\mu} \int_0^{\mu} [c_p(\lambda)]_{gs} d\lambda \tag{2.95}$$

where, $\mu = A/x_c$

$$c_p(\mu) = \frac{1}{\mu}\left[\int_0^1 c_o d\lambda + \int_1^{\mu} \{c_o + (\alpha + \frac{1-\alpha}{\lambda})^{-1/2} (\frac{4(1-\alpha)}{\pi\lambda^2} (m\omega_o)(\lambda-1))\} d\lambda\right]$$

$$= \frac{1}{\mu} \int_0^{\mu} c_o d\lambda + \frac{4(1-\alpha)}{\pi\mu} (m\omega_o) \int_1^{\mu} (\alpha + \frac{1-\alpha}{\lambda})^{-1/2} (\frac{\lambda-1}{\lambda^2}) d\lambda \tag{2.96}$$

But

$$(\alpha + \frac{1-\alpha}{\lambda})^{-1/2} = \sqrt{\frac{\lambda}{\alpha(\lambda-1)+1}} \tag{2.97}$$

Hence,

$$c_p(\mu) = c_o + \frac{4(1-\alpha)}{\pi\mu}(m\omega_o) \int_1^{\mu} \frac{(\lambda-1)}{\lambda^{3/2}\sqrt{\alpha(\lambda-1)+1}} d\lambda \qquad (2.98)$$

Equations (2.93), (2.98) together define the properties of the substitute non-hysteretic system.

2.8 AVERAGE STIFFNESS & ENERGY (ASE)

This method was proposed by Gates (12). In this extension of geometric stiffness method, the effective stiffness is obtained in the same way as in ASD. However, the equivalent damping is obtained by averaging the energies dissipated. This is accomplished as follows

$$\Delta W(A) = \frac{1}{A}\int_0^A \Delta W(a)da \qquad (2.99)$$

Again, the effective damping is determined by using the criteria expressed in equation (2.72), the difference being that here the average of the dissipated energies is considered. This is described by equation (2.99). This approach leads to the following equation

$$c_p = c_o\left(\frac{\omega_o}{\omega_p}\right) + \frac{6(1-\alpha)}{\pi\mu^3}\left(\frac{k_o}{\omega_p}\right)(\mu - 1)^2$$

$$= \left(\frac{\omega_o}{\omega_p}\right)\left[c_o + \frac{6(1-\alpha)}{\pi\mu^3}(m\omega_o)(\mu - 1)^2\right] \qquad (2.100)$$

Substituting $k_o = m\omega_o$, we get

$$c_p = \left[\frac{(1-\alpha)}{\mu}(1 + \ell n\mu) + \alpha\right]^{-1/2}\left\{c_o + \frac{6(1-\alpha)}{\pi\mu^3}(m\omega_o)(\mu - 1)^2\right\} \qquad (2.101)$$

As mentioned earlier, the effective stiffness, $k_p(A)$, is given by equation (2.93).

This method is particularly suitable for deteriorating systems. The effective properties of the equivalent non-hysteretic system are obtained by averaging the values associated with the upper and lower loci of response maxima. However, the results derived above are valid only for elasto-plastic and bilinear, hysteretic systems.

It should be noted that in all the above methods, the values of the effective stiffness and damping are the same as those of the original system if the absolute value of the displacement is smaller than the yield displacement. Hence, the functions $k_p(x)$ and $c_p(x)$ are not continuous and this must be properly accounted for in the numerical integration scheme described in section 2.3. Fig. 6 shows a typical representation of the effective non-hysteretic properties as defined by the various models considered in this study.

2.9 IMPLEMENTATION OF EQUIVALENT LINEAR APPROACH

A computer program was developed to implement the methods presented in this chapter. For a given set of system parameters such as natural frequency, damping ratio and yield displacement the program computes the response predicted by each method. This is accomplished by finding the properties of the equivalent linear system corresponding to the non-hysteretic model of each method. The program uses the available elastic spectra to determine the response of the equivalent linear system.

The results are obtained in an iterative fashion. First the properties of the equivalent linear system are first assumed to be certain values and then depending on the assumed value of the peak factor, the value of standard deviation σ_x is determined. Based on this estimation of the standard deviation, the new values of equivalent properties are obtained. The program iterates until the criteria for convergence are met with. An iteration limit is also specified to avoid any possible non-convergent case.

It may be noted that the response prediction in each method depends on the value of the peak factor assumed. Due to the nature of criteria on which these models are based, the adoption of a proper peak factor in each case is not an easy task. A certain judgement can however be exercised in this regard and this part is discussed in chapter 4 in more details. Vanmarcke has proposed a way of computing the peak factor for known spectral characteristics and the given system properties (43). A modified approach based on Vanmarcke's formulation (38) for peak factor was also used. The computational algorithm for the implementation of the equivalent linear approach can be summarized by the following steps

1. Input the system parameters viz ω_o, the natural frequency, β_o, the damping ratio, α, the ratio of the secondary stiffness to the primary stiffness and x_c, the yield displacement level. A fixed peak factor value should be stipulated unless Vanmarcke's formulation is being used.

2. Assume the values for ω_e and β_e, the properties of the linearized system. If Vanmarcke's formulation is to be used, then an iterative approach may be used to solve for the value of the peak factor corresponding to the above assumed values. After this, the steps for either the fixed peak factor or Vanmacke's peak factor approach is the same.
3. Read the spectral values corresponding to the present values of linear properties.
4. Compute the σ_x, standard deviation of relative displacement response corresponding to the assumed set of linear properties. It is obtained by dividing the mean spectral displacement by the value of the peak factor.
5. Using the desired non-hysteretic model and the proposed equivalent linear method, compute the new estimates for ω_e and β_e. These depend on the current value of σ_x, the standard deviation.
6. Check for a simultaneous convergence of ω_e and β_e to a desired level of accuracy. Repeat steps three through six until convergence occurs.

The results of the algorithms developed in this chapter are discussed in chapter 4.

Chapter III

TIME-HISTORY ANALYSIS

3.1 INTRODUCTION

In this chapter, exact solution algorithms for elastic, elasto-plastic and bilinear hysteretic (BLH) systems are presented. A time-history analysis scheme based on Newmark's method is also presented. The results of this (approximate) method can be used to cross-check the formulation and the results of the exact solutions. Development of the computer program to implement these algorithms is also discussed. Various results generated using the exact algorithm are thus made available for checking the accuracy of the methods presented in chapter 2.

For the purpose of equivalent linear analysis, it is necessary to construct a wide range of elastic response spectra as the basic reference data set. The whole purpose of equivalent linearization is to be able to predict the response of a given inelastic system by defining its equivalent linear system. The response of the inelastic system is approximately equal to that of its equivalent linear system, which is obtained by reading the appropriate elastic response spectrum.

3.2 LINEAR ELASTIC SYSTEMS

The equation of motion for a single-degree-of-freedom, elastic oscillator is given by

$$m\ddot{x} + c\dot{x} + kx = -ma(t) \tag{3.1}$$

where, 'x' is the relative displacement of the oscillator with respect to its moving base; $\dot{x}$ and $\ddot{x}$ are the relative velocity and relative acceleration respectively. m, c and k are respectively the mass, viscous damping coefficient and the (constant) stiffness of the spring. a(t) is the base acceleration at instant t. Dividing each term of equation (2.2) by m, we can write the following standard equation

$$\ddot{x} + 2\beta_0\omega_0\dot{x} + \omega_0^2 x = -a(t) \tag{3.2}$$

where, $\omega_0 = k/m$, the natural (circular) frequency of the oscillator, $\beta_0 = c/(2\omega_0 m) = c/c_{cr}$, ratio of the actual damping to the critical damping in the system. Critical damping is defined as the one which removes all vibration of the oscillator.

If we assume that the base acceleration varies linearly between the instances of two consecutive readings A_i and A_{i+1}, then we can express the response at time t_{i+1} in terms of the (known) response at time t_i. This exact step-wise solution scheme was presented by Nigam and Jennings (30,31). Above result can be obtained using the convolution integral approach to get the particular solution. Also, x_i and $\dot{x}_i$ are treated as the initial conditions. Denoting $h=(t_{i+1}-t_i)$, (constant) time interval between consecutive readings, then the results of Nigam and Jennings (30,31) can be expressed in a matrix form as follows

$$\begin{Bmatrix} x \\ \dot{x} \end{Bmatrix}_{i+1} = \begin{bmatrix} a_{11} & a_{12} \\ a_{21} & a_{22} \end{bmatrix} \begin{Bmatrix} x \\ \dot{x} \end{Bmatrix}_i + \begin{bmatrix} b_{11} & b_{12} \\ b_{21} & b_{22} \end{bmatrix} \begin{Bmatrix} A_i \\ A_{i+1} \end{Bmatrix} \tag{3.3}$$

where, the entries of matrices A and B are given by Nigam and Jennings (30,31), but they are repeated here for a ready reference.

$$a_{11} = e^{-\beta_0\omega_0 h}\left\{\frac{\beta_0}{\sqrt{1-\beta_0^2}}\sin(\omega_{dh}) + \cos(\omega_{dh})\right\}$$

$$a_{12} = \frac{e^{-\beta_0\omega_0 h}}{\omega_d h}\sin(\omega_d h)$$

$$a_{21} = \frac{\omega_0}{\sqrt{1-\beta_0^2}}\, e^{-\beta_0\omega_0 h}\sin(\omega_d h)$$

$$a_{22} = e^{-\beta_0\omega_0 h}\left\{\cos(\omega_d h) - \frac{\beta_0}{\sqrt{1-\beta_0^2}}\sin(\omega_d h)\right\}$$

$$b_{11} = e^{-\beta_0\omega_0 h}\left\{\left(\frac{2\beta_0^2-1}{\omega_0^2 h} + \frac{\beta_0}{\omega_0}\right)\frac{\sin(\omega_d h)}{\omega_d} + \left(\frac{2\beta_0}{\omega_0^3 h} + \frac{1}{\omega_0^2}\right)\cos(\omega_d h)\right\} - \frac{2\beta_0}{\omega_0^3 h} \tag{3.4}$$

$$b_{12} = -e^{-\beta_0\omega_0 h}\left\{\left(\frac{2\beta_0^2-1}{\omega_0^2 h}\right)\frac{\sin(w_d h)}{\omega_d} + \frac{2\beta_0}{\omega_0^3 h}\cos(\omega_d h)\right\} - \frac{1}{\omega_0^2} + \frac{2\beta_0}{\omega_0^3 h}$$

$$b_{21} = e^{-\beta_0\omega_0 h}\left\{\left(\frac{2\beta_0^2-1}{\omega_0^2 h} + \frac{\beta_0}{\omega_0}\right)\left[\cos(\omega_d h) - \frac{\beta_0}{\sqrt{1-\beta_0^2}}\sin(\omega_d h)\right]\right.$$

$$- \left(\frac{2\beta_0^{2} - \omega_0 h}{\omega_0^3 h}\right)[\omega_d \sin(\omega_d h) + \beta_0 \omega_0 \cos(\omega_d h)] \Big\} + \frac{1}{\omega_0^2 h}$$

$$b_{22} = -e^{-\beta_0 \omega_0 h} \Big\{ \left(\frac{2\beta_0^2 - 1}{\omega_0^2 h}\right)[\cos(\omega_d h) - \frac{\beta_0}{\sqrt{1 - \beta_0^2}} \sin(\omega_d h)] - \frac{2\beta_0}{\omega_0^3 h} [\omega_d \sin(\omega_d h)$$

$$+ \beta_0 \omega_0 \cos(\omega_d h)] \Big\} - \frac{1}{\omega_0^2 h}$$

Note that

$$\omega_d = \omega_0 \sqrt{1 - \beta_0^2} \tag{3.5}$$

It may be noted that 'h' need not be a constant; however, a changing value of h would necessitate the computation of entries of matrices A and B whenever such a change is made. It should also be noted that these results are accurate irrespective of the value of h, the size of the time step.

A computer program that implements above algorithm was developed. Sharma, Singh, etc (37), generated a wide range of elastic response spectra using that program. In his work, the periods considered ranged from .02 seconds to 5.00 seconds and the damping coefficients ranged from .005 to .500. The spectra were generated for ensembles of 12 seconds, 15 seconds and 30 seconds time histories. The 15 second spectra are used in this work. They correspond to a maximum ground acceleration in the neighborhood of .10G. For the case of linear behavior, the spectral values for linearly amplified ground motion are simply obtained by multiplying the values in the available records by the same (constant) amplification factor. A simple log-log interpolation was used to obtain the response spectrum values for frequencies and damping ratios other than the ones used to define spectra.

3.3 ELASTO-PLASTIC & BILINEAR HYSTERETIC SYSTEMS

Systems considered in this work have the following general form of equation of motion

$$m\ddot{x} + c\dot{x} + f(x,\dot{x}) = -ma(t) \tag{3.6}$$

It can be easily seen that the nonlinearity considered is of material type (unlike the geometric one). Clearly, the hysteresis is caused due to velocity dependence of the restoring force in the spring. Referring to figures 3 and 4, it can be seen that in both cases, the force-displacement relationships along paths 1 and 3 are given by

$$f_1(x,\dot{x}) = k_0 x \tag{3.7}$$

and

$$f_3(x,\dot{x}) = k_0(x - c) \tag{3.8}$$

where 'c' is the X-intercept of line 3 as seen in figures 3 and 4. Along lines 2 and 4, the restoring force is given by

$$f_{2,4}(x,\dot{x}) = F_c\left(\frac{\dot{x}}{|\dot{x}|}\right) \qquad \text{elasto-plastic} \tag{3.9}$$

and

$$f_{2,4}(x,\dot{x}) = F_c \frac{\dot{x}}{|\dot{x}|} + \alpha k_0 \left(x - x_c \frac{\dot{x}}{|\dot{x}|}\right) \quad \text{bilinear} \tag{3.10}$$

Note that

$$FC = k_0 x_c \tag{3.11}$$

It is easy to observe that the solution along path 1 is the same as the one given by equations (3.3), (3.4) and (3.5). Along path 3, we can write the equation of motion as

$$\ddot{x} + 2\beta_0 \omega_0 \dot{x} + \omega_0^2 (x - c) = -a(t) \tag{3.12}$$

this may be rewritten as

$$\ddot{x} + 2\beta_0 \omega_0 \dot{x} + \omega_0^2 x = - \bar{a}(t) \tag{3.13}$$

where,

$$\bar{a}(t) = - \left[a(t) - \omega_0^2 c\right] \tag{3.14}$$

Clearly, equation (3.3) is applicable to the above form of the equation of motion, thus the solution for response along path 3 can be expressed in a matrix form as follows

$$\begin{Bmatrix} x \\ \dot{x} \end{Bmatrix}_{i+1} = \begin{bmatrix} a_{11} & a_{12} \\ a_{21} & a_{22} \end{bmatrix} \begin{Bmatrix} x \\ \dot{x} \end{Bmatrix}_i + \begin{bmatrix} b_{11} & b_{12} \\ b_{21} & b_{22} \end{bmatrix} \begin{Bmatrix} \bar{A}_i \\ \bar{A}_{i+1} \end{Bmatrix} \tag{3.15}$$

where,

$$\bar{A}_i = \left[A_i - \omega_0^2 c\right] \tag{3.16a}$$

and

$$\bar{A}_{i+1} = [A_{i+1} - \omega_0^2 c] \tag{3.16b}$$

Equations (3.15) and (3.16) are used to obtain the response along path 3. Note that the entries of matrices A and B are the same as defined earlier by equations (3.4) and (3.5).

For elasto-plastic systems, the equation of motion along path 2 and 4 can be written as

$$m\ddot{x} + cx + F_c \frac{\dot{x}}{|\dot{x}|} = - ma(t) \tag{3.17}$$

In the above equation F is the spring force corresponding to either positive or negative yield displacement. In particular, the positive and the negative yield displacements may be denoted as F_{cp} and F_{cn} respectively. Thus equation (3.17) is equivalent to the following two differential equations.

$$m\ddot{x} + c\dot{x} + F_{cp} = -ma(t) \tag{3.18a}$$

and

$$m\ddot{x} + c\dot{x} + F_{cn} = - ma(t) \tag{3.18b}$$

where,

$$F_{cp} = k_0 x_c, \; F_{cn} = -k_0 x_c \tag{3.19}$$

Clearly, both the equations labelled as (3.18) are equivalent as far as the solution procedure is concerned. Hence, we find the solution to the differential equation of following type

$$m\ddot{x} + c\dot{x} = - m[A_i + (\frac{A_{i+1} - A_i}{h})t] - F_c \; ; \; 0 < t < h \qquad (3.20)$$

Dividing each term of above equation by m, we get

$$\ddot{x} + 2\beta_o\omega_o\dot{x} = - [A_c + A_i + (\frac{A_{i+1} - A_i}{h})t] \qquad (3.21)$$

where,

$$A_c = F_c/m = \omega_o^2 x_c \frac{\dot{x}_i}{|\dot{x}_i|} \qquad (3.22)$$

The homogeneous solution to above differential is found to be as follows

$$x_h = c_1 + c_2 e^{-2\beta_o\omega_o t} \qquad (3.23)$$

Using the method of undetermined coefficients, we get the particular solution as

$$x_p = - (\frac{A_{i+1} - A_i}{4\beta_o\omega_o h})t^2 + [\frac{A_{i+1} - A_i}{4\beta_o^2\omega_o^2 h} - \frac{ACG + A_i}{2\beta_o\omega_o}]t - (\frac{A_{i+1} - A_i}{4\beta_o\omega_o h})t^2 \qquad (3.24)$$

Now, $x=x_h+x_p$, hence, substituting equations (3.23) and (3.24), we get

$$x = c_1 + c_2 e^{-2\beta_o\omega_o t} + [\frac{A_{i+1} - A_i}{4\beta_o^2\omega_o^2 h} - \frac{ACG + A_i}{2\beta_o\omega_o}]t - (\frac{A_{i+1} - A_i}{4\beta_o\omega_o h})t^2 \qquad (3.25)$$

Differentiating (3.25), we get

$$\dot{x} = - 2\beta_o\omega_o c_2 e^{-2\beta_o\omega_o t} + (\frac{A_{i+1} - A_i}{4\beta_o^2\omega_o^2 h}) - (\frac{ACG + A_i}{2\beta_o\omega_o}) - (\frac{A_{i+1} - A_i}{2\beta_o\omega_o h})t \qquad (3.26)$$

The above solution is subject to the following initial conditions

$$x(t=0) = x_i \qquad \text{and} \qquad \dot{x}(t=0) = \dot{x}_i \tag{3.27}$$

Applying these initial conditions, we obtain the following values of the boundary terms

$$c_2 = -\frac{\dot{x}_i}{2\beta_o\omega_o} + \frac{A_{i+1} - A_i}{8\beta_o^3\omega_o^3 h} - \frac{ACG + A_i}{4\beta_o^2\omega_o^2} \tag{3.28}$$

and

$$c_1 = x_i + \frac{\dot{x}_i}{2\beta_o\omega_o} - \frac{A_{i+1} - A_i}{8\beta_o^3\omega_o^3 h} + \frac{ACG + A_i}{4\beta_o^2\omega_o^2} \tag{3.29}$$

After substituting equations (3.28) and (3.29) in (3.25) and (3.26) and reorganizing the terms, we can write the final expressions in following form (with t=h for the response at time t_{i+1})

$$\begin{Bmatrix} x \\ \dot{x} \end{Bmatrix}_{i+1} = \begin{bmatrix} c_{11} & c_{12} \\ c_{21} & c_{22} \end{bmatrix} \begin{Bmatrix} x \\ \dot{x} \end{Bmatrix}_i + \begin{bmatrix} d_{11} & d_{12} \\ d_{21} & d_{22} \end{bmatrix} \begin{Bmatrix} A_i \\ A_{i+1} \end{Bmatrix} + \begin{Bmatrix} X_{pi} \\ V_{pi} \end{Bmatrix} \tag{3.30}$$

where,

$$c_{11} = 1.0$$

$$c_{12} = \frac{1}{2\beta_o\omega_o}\left(1 - e^{-2\beta_o\omega_o h}\right)$$

$$c_{21} = 0.0$$

$$c_{22} = e^{-2\beta_o\omega_o h}$$

$$d_{11} = \frac{1}{4\beta_o\omega_o}\left\{\frac{1}{2\beta_o^2\omega_o^2 h}\left(-e^{-2\beta_o\omega_o h}\right) + \frac{1}{\beta_o\omega_o} + \frac{1}{2\beta_o^2\omega_o^2 h} - h\right\}$$

$$d_{12} = \frac{1}{4\beta_o\omega_o}\left\{\frac{1}{2\beta_o^2\omega_o^2 h}\left(e^{-2\beta_o\omega_o h} - 1\right) + \frac{1}{\beta_o\omega_o} - h\right\} \tag{3.31}$$

$$d_{21} = \frac{1}{2\beta_o\omega_o}\left\{e^{-2\beta_o\omega_o h} \ \frac{1}{2\beta_o\omega_o h} + 1 \ - \frac{1}{2\beta_o\omega_o h}\right\}$$

$$d_{22} = \frac{1}{2\beta_o\omega_o}\left\{\frac{1}{2\beta_o\omega_o h}\left(1 - e^{-2\beta_o\omega_o h}\right) - 1\right\}$$

$$X_{\rho l} = \left[\frac{1}{2\beta_o\omega_o}\left\{\frac{1}{2\beta_o\omega_o}\left(1 - e^{-2\beta_o\omega_o h}\right) - h\right\}\right](A_c)$$

$$V_{pl} = \left[\frac{1}{2\beta_o\omega_o}\left(e^{-2\beta_o\omega_o h} - 1\right)\right](A_c)$$

Equations (3.30) and (3.31) define the solution for response along paths 2 and 4 of an elasto-plastic, hysteretic oscillator.

Considering a bilinear, hysteretic system ($\alpha \neq 0$), we can write the following equation of motion along paths 2 and 4

$$m\ddot{x} + c\dot{x} + F_c \frac{\dot{x}}{|\dot{x}|} + \alpha k_o\left(x - x_c \frac{\dot{x}}{|\dot{x}|}\right) = - ma(t) \qquad (3.32)$$

or

$$m\ddot{x} + c\dot{x} + (\alpha k_o)x = - ma(t) - F_c \frac{\dot{x}}{|\dot{x}|}(1 - \alpha) \qquad (3.33)$$

Similar to equations (3.18), above equation is equivalent to two ordinary differential equations. Hence, as before, we can consider a following form of differential equation to solve for the response

$$\ddot{x} + 2\beta^*\omega^*\dot{x} + \omega^{*2}x = - \bar{a}(t) \qquad (3.34)$$

where, the quantities marked with asterisk are given as

$$\omega^* = \sqrt{\alpha k_o/m} = \omega_o\sqrt{\alpha} \qquad (3.35)$$

and

$$\beta^* = c/(2\omega^* m) = \beta_0/\sqrt{\alpha} \tag{3.36}$$

Also,

$$\bar{a}(t) = a(t) + \omega_0^2 x_c (1 - \alpha) \frac{\dot{x}}{|\dot{x}|} \tag{3.37}$$

Note that

$$(2\beta_0\omega_0) = (2\beta^*\omega^*) = c/m \tag{3.38}$$

Comparing equations (3.2) and (3.34), we observe that the solution to equation (3.34) can be expressed in a form similar to equation (3.3) as follows

$$\begin{Bmatrix} x \\ \dot{x} \end{Bmatrix}_{i+1} = \begin{bmatrix} e_{11} & e_{12} \\ e_{21} & e_{22} \end{bmatrix} \begin{Bmatrix} x \\ \dot{x} \end{Bmatrix}_i + \begin{bmatrix} f_{11} & f_{12} \\ f_{12} & f_{22} \end{bmatrix} \begin{Bmatrix} \bar{A}_i \\ \bar{A}_{i+1} \end{Bmatrix} \tag{3.39}$$

where,

$$e_{11} = e^{\beta^*\omega^* h} \left\{\frac{\beta^*}{\sqrt{1 - \beta^{*2}}} \sin(\omega_d^* h) + \cos(\omega_d^* h)\right\}$$

$$e_{12} = \frac{e^{-\beta^*\omega^* h}}{\omega_d^* h} \sin(\omega_d^* h)$$

$$e_{21} = \frac{\omega^*}{\sqrt{1 - \beta^{*2}}} e^{-\beta^*\omega^* h} \sin(\omega_d^* h)$$

$$e_{22} = e^{-\beta^*\omega^* h}\left\{\cos(\omega_d^* h) - \frac{\beta^*}{\sqrt{1 - \beta^{*2}}} \sin(\omega_d^* h)\right\} \tag{3.40}$$

$$f_{11} = e^{-\beta^*\omega^* h}\Big\{\Big(\frac{2\beta^{*2} - 1}{\omega^{*2}h} + \frac{\beta^*}{\omega^*}\Big)\frac{\sin(\omega_d^* h)}{\omega_d^*} + \Big(\frac{2\beta^*}{\omega^{*3}h} + \frac{1}{\omega^{*2}}\Big)\cos(\omega_d^* h)\Big\} - \frac{2\beta^*}{\omega^{*3}h}$$

$$f_{12} = -e^{\beta^*\omega^* h}\Big\{\Big(\frac{2\beta^{*2} - 1}{\omega^{*2}h}\Big)\frac{\sin(\omega_d^* h)}{\omega_d^*} + \frac{2\beta^*}{\omega^{*3}_{h}}\cos(\omega_d^* h)\Big\} - \frac{1}{\omega^{*2}} + \frac{2\beta^*}{\omega^{*3}h}$$

$$f_{21} = e^{-\beta^*\omega^* h}\Big\{\Big(\frac{2\beta^{*2} - 1}{\omega^{*2}h} + \frac{\beta^*}{\omega^*}\Big)\Big[\cos(\omega_d^* h) - \frac{\beta^*}{\sqrt{1 - \beta^{*2}}}\sin(\omega_d^* h)\Big]$$

$$- \Big(\frac{2\beta^*}{\omega^{*3}h} + \frac{1}{\omega^{*2}}\Big)\Big[\omega_d^*\sin(\omega_d h) + \beta^*\omega^*\cos(\omega_d^* h)\Big]\Big\} + \frac{1}{\omega^{*2}h}$$

$$f_{22} = -e^{\beta^*\omega^* h}\Big\{\Big(\frac{2\beta^{*2} - 1}{\omega^{*2}h}\Big)\Big[\cos(\omega_d^* h) - \frac{\beta^*}{\sqrt{1 - \beta^{*2}}}\sin(\omega_d^* h)\Big]$$

$$- \frac{2\beta^*}{\omega^{*3}h}\Big[\omega_d^*\sin(\omega_d^* h) + \beta^*\omega^*\cos(\omega_d^* h)\Big]\Big\} - \frac{1}{\omega^{*2}h}$$

Note that

$$\omega_d^* = \omega^*\sqrt{1 - \beta^{*2}} \tag{3.41}$$

Also,

$$\bar{A}_i = A_i + \omega_0^2(xc)(1 - \alpha)\frac{\dot{x}_i}{|\dot{x}_i|} \tag{3.42a}$$

and

$$\bar{A}_{i+1} = A_{i+1} + \omega_0^2(xc)(1 - \alpha)\frac{\dot{x}_i}{|\dot{x}_i|} \tag{3.42b}$$

Equations (3.40), (3.41) and (3.42) define the solution to the response along paths 2 and 4 for a bilinear, hysteretic systems.

Radoshycka (33) did similar work for his Master's thesis at Rice University. More recently, Nau (25) presented essentially the same results as presented above. It is however, mentioned here that the author was unaware of these works at the time the above solution was developed. It was observed that the formulation developed in this work is consistent with the ones derived by Radoshycka and Nau.

3.4 TIME-HISTORY ANALYSIS USING APPROXIMATE METHODS

As mentioned earlier, it is generally not possible to develop the exact solution to the response of systems with any general type of nonlinear and/or hysteretic behavior. A time-history analysis of such response is sometimes necessary for a detailed study of the response history. Various time-history analysis schemes may also be used for the purpose of verification of the results obtained using other methods. Newmark was one of the pioneers in developing such methods. These are often referred to as the direct integration methods, since the equation of motion is integrated at each instant to obtain the response at that instant. The relative acceleration in the response is assumed to be either linearly varying or constant during each incremental time-step. In case of nonlinear problems, an improvisation over Newmark's original method can be done by a tangent stiffness approach to arrive at a better estimate of the stiffness (or stiffness matrix for a multi-degree of freedom system) at each instant.

3.5 IMPLEMENTATION OF TIME-HISTORY ANALYSIS METHODS

A computer program was developed to implement the exact solution algorithms presented earlier. This program is capable of solving for perfectly elastic systems as well as elasto-plastic and bilinear hysteretic systems. The program incorporates the following advantages of the exact solution

1. The response is accurate regardless of the size of the time-step.
2. The times at which the system behavior changes from one path to another can be located accurately.

As mentioned earlier, the size of time-step is governed by the spacing of ground acceleration readings and hence, the first advantage is generally rendered insignificant, since in case of nonlinear systems, it is necessary to compute the response at all known acceleration readings as the response is dependent on the path between the instances of any two readings under consideration. This is in contrast to the linear systems, where the response at any given time depends only on the values at the beginning of the time-step and the ground acceleration reading at that time.

The program produces results for given values of the natural frequency, damping ratio, ratio of the secondary to the primary stiffness and the magnitude of yield displacements (positive and negative). At each time-step, the properties of the system are inspected to determine the path it is following at such instant. A

Paz(32) has presented an algorithm to compute the response of any general nonlinear single-degree-of-freedom system. It is based on Newmark's method and corresponds to the case of the parameter, β = 1/6. The relative acceleration of the oscillator is assumed to vary linearly during each time interval as shown in figure 7. The approximate solution can be described by the following equations

$$\Delta x_i = \frac{m\{-\Delta A_i + \frac{6}{h}\dot{x}_i + 3\ddot{x}_i\} + c\{3\dot{x}_i + \frac{h}{2}\ddot{x}_i\}}{(k_i + \frac{6m}{h^2} + \frac{3c}{h})} \tag{3.47}$$

$$\Delta\ddot{x}_i = \frac{6}{h^2}\Delta x_i - \frac{6}{h}\dot{x}_i - 3\ddot{x}_i \tag{3.48}$$

and

$$\Delta\dot{x}_i = \frac{3}{h}\Delta x_i - 3\dot{x}_i - \frac{h}{2}\ddot{x}_i \tag{3.49}$$

Finally the response at time t_{i+1} is given as

$$x_{i+1} = x_i + \Delta x_i \tag{3.50}$$

and

$$\dot{x}_{i+1} = \dot{x}_i + \Delta\dot{x}_i \tag{3.51}$$

Equations (3.48) and (3.49) together define the response of any general nonlinear system.

change of path (fig. 4) indicates change in the system behavior. Every time such change occurs, the program invokes the appropriate kink locater routine to determine the exact time at which the system changes its behavior. Thus the response history for relative displacement, relative velocity, relative and absolute acceleration and the spring force (if desired) is generated during the execution of this program. However, in the context of this thesis, one would only be interested in the response characteristics such as the mean and standard deviation of response maxima, root mean square values, etc. As such, these are the outputs produced by this program with an option for printing the response history, if desired.

A computer program based on Paz's algorithm was also developed for the purpose of verification of the results obtained with the program employing the exact solution algorithms. In this case, it is necessary that the size of the time-step be very small to ensure accurate results. In this case the size of time-step was taken to be the same as the spacing of consecutive ground acceleration readings (0.002 seconds), which is small enough to ensure good accuracy.

The above mentioned computer programs were used to create elastic response spectra and a few sample spectra for the hysteretic oscillators. The exact solution results were used as reference for testing the accuracy of the results obtained using the methods presented in chapter 3. The results from chapter 3 are presented in chapter 4.

Chapter IV

RESULTS AND CONCLUSIONS

4.1 SEISMIC INPUT

For the purpose of this work, ensembles of artificially generated ground response spectra (acceleration time histories) were used. It is necessary that the seismic input be defined in terms of ground response spectra curves for the sake of consistency. It was thought better to artificially generate the ensembles of time histories (with certain frequency and intensity characteristics) for the use in time history analysis and for the generation of elastic response spectra, since it is difficult to find authentic ground acceleration records having consistent energy dissipation characteristics. Variety of methods have been proposed in this context (42,44).

The base accelerations are assumed to be represented as follows

$$\ddot{x}_g(t) = \ddot{x}_s(t)e(t) \tag{4.1}$$

in which $x_g(t)$ is the base acceleration, $x_s(t)$ is a stochastically generated time history motion; and e(t) is an intensity modulation function. The modulation function causes the (artificial) input to be of a character similar to the actual earthquakes (consisting of a build-up phase, strong-motion phase and the decaying phase). The stationary nature of $x_s(t)$ is destroyed since it is multiplied by the modulation function. Hence, the actual input used is of non-stationary nature.

$x_s(t)$ is characterized by a modified Kanai-Tajimi type of spectral density function in which more terms are added to get a broad band effect.

$$\Phi_s(\omega) = \sum_{i=1}^{3} S_i \frac{\omega_i^4 + 4\beta_i^2\omega_i^2\omega^2}{(\omega_i^2 - \omega^2)^2 + 4\beta_i^2\omega_i^2\omega^2} \tag{4.2}$$

Table 1 tabulates the parameters S_i, ω_i, and β_i of the above spectral density function (see ref. 39). A standard technique, originally proposed by Rice (35) is used to generate the sample acceleration time-history functions corresponding to the above density function. As mentioned earlier, all these time-history functions are then rendered non-stationary with the use of rather arbitrarily selected envelope functions. A further modification for base line correction is carried out so that any erroneous long period effects occuring during the generation process are removed. The importance of this has been investigated by Chopra and Lopez (10) in reference to inelastic response of structures. The ensembles used in this work were generated by Singh and Ashtiany (39).

A total of 75 earthquake time histories were generated using above procedure. Each record is of 15 seconds duration. In a similar manner, 100 records of 12 seconds duration each and 39 records of 30 seconds duration each were generated. The maximum value of ground acceleration for all the records is in the neighborhood of .1G.

In order to cause large displacement response beyond the elastic range, the same earthquake time histories were used by applying amplification factors of 2 over each reading in the ground acceleration records. Due to this, the elastic response spectra are merely amplified by the same factor, however, the effect on inelastic systems can not be predicted in such a simple manner.

It is necessary to construct a wide range of elastic response spectra as the basic reference data set. The whole purpose of equivalent linearization method is to be able to predict the response of a given inelastic system by defining its equivalent linear properties. The response of the inelastic system is approximately equal to that of its equivalent linear system; which is obtained by reading the appropriate elastic response spectrum.

4.2 GENERATION OF ELASTIC RESPONSE SPECTRA

The available response spectra were extended for higher values of periods and damping. Use of the equivalent linear analysis methods may give rise to large values of equivalent damping ratio and/or period, out of the range of the available spectra. This necessitated the generation of elastic spectra covering a wide range periods and damping ratios.

A simple computer program was written to generate the elastic response spectra upto a range of 15 seconds period and 0.90 damping ratio. Results by Nigam and Jennings (30,31) were used in this program. It computes mean and standard deviation of the maximum response quantities such as relative displacement, relative velocity, relative acceleration and absolute acceleration. Since the results are accurate despite the size of the time-step, a comparatively larger time-step was used to affect computational savings.

In Figures 4.10 through 4.13, the elastic response spectra are represented by the uppermost of the curves, corresponding to a ductility ratio of one (no yielding). The famous enveloping effect at intermediate frequency range as observed in the Newmark - Blume - Kapoor spectra (26) can be seen present in these plots, too.

4.3 GENERATION OF INELASTIC RESPONSE SPECTRA

Response spectra were generated for an elasto-plastic system with damping ratio of 0.05. For this, the frequency was varied between 0.20 cps to 35 cps. The 21 values of frequencies considered in this range are listed in Table 1. The ensemble of 75 time-histories of 15 seconds duration each was used for this work. An amplification factor of 2.0 was used for each ground acceleration reading in all time-histories. This was done so as to affect a higher ductility ratio at values of yield displacements which were not too small. The computer program mentioned in section 3.5 was used to achieve the results. A time-step of 0.002 seconds was used for the purpose of accuracy. The times at which the system changes its behavior during its response history were traced accurately with the use of this program. Some of the results of were validated by a simpler computer program based on Paz's algorithm.

The procedure to obtain the yield displacement corresponding to a desired level of ductility is described by Riddell (36). Since a given level of yield displacement is unlikely to produce the response at a specified ductility level, the program was used to compute the statistical response characteristics for a range of yield displacements depending on the frequency of the oscillator. An inspection of the elastic response spectra for relative displacement is helpful for this purpose. Corresponding to each yield displacement level, the computer program computes the mean and standard deviation of the maximum response quantities of each time history. The effective root mean square value is taken as the maximum of the various root mean square values (along the time axis). Each such value is in turn computed by the following formula

$$RMS(q(t)) = \sqrt{\frac{\sum_{i=1}^{N} q_i^2(t)}{N}} \qquad (4.3)$$

where, q(t) = the value of response quantity at time t and N = number of time histories

It may be noted here that 't' in this case is a discrete variable in this case is a discrete variable with increments of 0.002 seconds. Thus there are 7500 such RMS values along the time axis. Finally, the maximum RMS values are given as

$$RMS(q) = \text{Maximum}\left[\sqrt{\frac{\sum_{i=1}^{N} q_i^2(t)}{N}}\right] ; \quad j = 1,\ 7500 \qquad (4.4)$$

μ, the ductility ratio and $P_f(q)$, the peak factor are defined as

$$\mu = \frac{\text{Maximum Relative Displacement}}{\text{Yield Displacement}} \tag{4.5}$$

and

$$P_f(q) = \frac{\text{Maximum value of Response, } q}{\text{RMS}(q)} \tag{4.6}$$

In the above equations, the 'maximum' may be taken as the mean of the maxima corresponding to all the time-histories, or it may be taken as (mean plus some constant times the standard deviation) of such maxima. For example, if we assume a stationary Gaussian response, the mean would correspond to a probability of exceedance of 50 %. The program gives the ductility ratios and peak factors corresponding to the mean and (mean plus one standard deviation). Again, the response quantities considered were relative displacement, relative velocity, relative acceleration and absolute acceleration.

A run of the program for given values of yield displacements for a fixed value of frequency and damping ratio would thus yield a range of ductility values corresponding to that set. A plot of yield displacement vs ductility ratio can then be made and the yield levels corresponding to the desired ductilities can be picked out by either graphical interpolation or simply by a linear interpolation scheme (see fig. 7-9). A graphical interpolation scheme was presented by Riddell

(36). For this work, linear interpolation was carried out between the appropriate pairs of consecutive readings to pick out the yield levels corresponding to ductility ratios of 2, 4, 5, 8, and 10. Corresponding values of other response quantities were also obtained by linear interpolation between the same pairs of consecutive records.

In most uses the dependance of ductility on the yield level is of monotonic nature. Thus, a decrease in the yield level generally leads to an increase in the ductility. However, this is not necessarily true. In particular, for elasto-plastic systems the displacement and velocity responses sometimes tend to accumulate. This means that for certain time-histories, it may happen that these responses become very large, thereby largely affecting the mean, standard deviation and the RMS values. This also disturbs the otherwise monotonic relationship between yield level and ductility. In order to overcome this problem, an arbitration procedure was incorporated in this program. Since most structural steel materials exhibit a strain-hardening behavior after some level of ductility (which in fact, can be idealized by a trilinear behavior, Ref. 1), an upper limiting value of ductility was prescribed for each computer run and the program would consider the maximum relative displacement as this upper limit times the yield level, in case it is detected that the displacement exceeds this upper limiting value. The selection of this upper limit was based on the remarks in Ref. 1.

Using this procedure, the response spectra were generated for ductility ratios of 2, 4, 5, 8 and 10 for elasto-plastic oscillators (α = 0) with damping ratio of 0.05. The spectra were generated for relative displacement, relative velocity, relative acceleration and absolute acceleration. Figures 10 through 13 represent these spectra.

4.4 OTHER TIME-HISTORY ANALYSIS RESULTS

A few runs were made for different values of α, the ratio of stiffnesses and p, the damping ratio. The main intention for this was to generate the exact results which can be used to judge the effectiveness of the equivalent linearization scheme with different non-hysteretic models.

The same computer program mentioned above was used for this purpose. A value of α other than zero was chosen which represents a BLH system and the program is capable of producing the same results for such a system with the same kind of accuracy.

4.5 RESULTS OF EQUIVALENT LINEARIZATION

The method of equivalent linearization used in this work is an indirect one, since the original hysteretic system is first modelled as a non-hysteretic one and then the equivalent linearization is carried out on such a model. Hence the results of these analyses depend on the criteria on which these models are based. As mentioned in chapter 2, a computer program was developed to implement these methods. The results are generated in an iterative fashion described earlier.

Besides the nature of the model itself, all the methods under this category depend on the value of peak factor used for their implementation. For the purpose of this work, a range of peak factors was used to inspect values of the peak factor that would give the best possible results. Runs were also made using the known values of peak factor obtained from the time-history analysis to see any correlation between the two corresponding results. Additionally, Vanmarcke's approach was also used to compute the results based on that formulation (43).

The results of time-history analysis were available for checking the accuracy of these methods. It was observed that the results of such a comparison define three zones of frequencies, depending on the kind of accuracy produced in each such zone. Characteristically, these zones almost coincide with the ones defined in the standard Newmark - Blume - Kapoor spectra (26). The results were found to be most consistent in the first frequency range (.25 cps-2.5 cps) and least consistent in the intermediate frequency range (2.5 cps-9.0 cps). All these trends are exemplified by the results tabulated in tables 3 through 17. It should be noted that the units are as follows : displacement - inches, velocity - ft/sec, acceleration - G units and frequency - cycles/second. The fact that a consistent peak factor can not be used to produce results of consistent accuracy range is exemplified in figures 14 through 16. These figures also indicate that one can not generate inelastic response spectra with the use of the models presented here, since the predicted response is dependent on numerous factors such as frequency, ductility range, assumed peak factor, etc. Tables 3-17 use the following abbreviations : PFC = Assumed Peak Factor, DRC = Predicted Ductility Ratio, RSVC = Predicted Relative Velocity, RSAC = Predicted Relative Acceleration, and ASAC = Predicted Absolute Acceleration.

For the case of elasto-plastic systems it was generally observed that these methods are satisfactory for low to moderate ductilities (upto μ=4 or 5). For higher ductilities, the relative displacement response is generally underestimated to a large extent. Also, the prediction of absolute acceleration and relative velocity response is comparatively overestimated in most cases. CCD was the only method most consistent in its results. However, as a general observation it may be said that these methods are not reliable for the task of producing a whole range of response spectra; they could only be used in certain ranges of frequency and ductility with some judgement for the selection of the peak factor value. It is possible that they be satisfactory for the prediction of the inelastic response of multi-degree of freedom structures.

Sample results for the BLH system response are also presented in the above mentioned tables. It was observed that the methods work much better for BLH systems. Again, the response prediction depends on the same factors mentioned earlier. In general, the results are most satisfactory for low to moderate ductilities. This observation is consistent with some conclusions drawn by Caughey (6).

Some conclusions along with a few explanatory remarks are presented in the next section.

4.6 CONCLUSIONS

1. The time-history analysis is the most reliable tool for response prediction. This fact was duly restated during this study. Different methods (whether approximate or exact) under this group stand as benchmarks for the purpose of verification of results obtained by various methods in use. The fact that the time-history analysis is computationally expensive was highlighted during this study. A comparison between the time-history analysis and the equivalent linear analyses showed that there is a 50-100 fold saving in computational time if the latter are used to estimate the response.

2. It was observed that for elasto-plastic systems, for frequencies 4 cps and above, the relative displacement response tends to become very large for some ground acceleration records. This is attributed to the fact that such a system has zero stiffness on the secondary path. The response follows this path as long as the relative velocity does not change its sign; occurence of which depends on the excitation input among other things. This problem is not encountered for BLH systems ($\alpha \neq 0$). However, the response is relatively unaffected for very low values of α. For large values of α (.20 onwards), the relative displacement response is considerably smaller compared to the one in the elasto-plastic case.

3. The approximate methods used in this study are satisfactory for low to moderate ductilities only, particularly for the case of elasto-plastic systems. This is due to the fact that all these methods assign some effective value of stiffness to the substitute non-hysteretic model, whereas the actual system responding along the secondary paths has a zero stiffness. This discrepancy becomes more pronounced for a highly ductile response wherein the system behavior is along the zero stiffness path for a considerable time; a fact which is not accounted for by the non-hysteretic models considered in this study.

4. The response prediction using the approximate methods of this group is more reliable for the case of BLH systems. This is due to the fact that such systems do have some stiffness after their yielding. As such there is no fundamental discrepancy in modelling them with some effective stiffness in their non-hysteretic models. It must however be mentioned that the accuracy of response prediction in this case would depend on the magnitude of the secondary stiffness. It is possible that these methods would overestimate the relative displacement response i such cases.

5. A comparison of individual methods shows that the HEL and GS methods produce similar results for low to moderate ductilities. A glance at fig. 6 explains the reason for this. Here, it can be

seen that both these yield almost identical results in that range of ductility. It was observed that CCD works satisfactory in most cases. This is possibly due to the fact that it considers the effective mass as changing as a function of the ductility level. Hence, even though it gives the same value of effective stiffness, it produces a smaller value of the effective damping coefficient. The last two methods were found to be most unsatisfactory in that they are very inconsistent. This is possibly due to the fact that they yield an effective system (and consequently the equivalent linear system) that has properties not very different from the original system. Thus one ends up with an equivalent linear system that is in the same frequency zone (generally defined by the Newmark - Blume - Kapoor spectra). Obviously, the response prediction in such a case is not much different from the one corresponding to the elastic response of the original system. In any case, these methods were deviced to model deteriorating systems unlike the ones considered under this study.

6. The accuracy of response prediction depends on the value of the peak factor assumed in the implementation of the approximate methods. It is thus necessary to exercise some judgement in the selection of a proper peak factor value. It is difficult to come up with a unique value in this regard, however, some general guidelines can be used for this purpose.

It is important to note that all the non-hysteretic models assume a harmonic response for a given amplitude level. The value of peak factor corresponding to harmonic response is 2 . If we assume that the amplitude of displacement is a slowly varying sine wave function of time (during the response history), then the corresponding value of the peak factor would be 2.0. Thus, it is reasonable to expect the proper peak factor value in the vicinity of this number. Another factor which governs this selection is the level of ductility. It can be observed from the time-history analysis that the actual value of the peak factor becomes smaller with an increase in the ductility level. This indicates that the displacement response is more dense (from the viewpoint of probability of actual occurence) near the maximum value, thus causing a reduced peak factor. A due consideration of this fact suggests that a value lower than 2.0 is more sensible for the cases where a large value of ductility ratio is expected. Also, the peak factor selection depends on the range of the frequency. For elasto-plastic systems, it was observed that the peak factor is much smaller for frequencies 4.0 onwards. This suggests a corresponding decrease in the adopted peak factor value in this range of frequency. Based on the runs made for various values of peak factor, some general guidelines were drawn for arriving at the proper peak factor. These are tabulated in table 18. It may be noted that the values for peak factor in case of CCD are somewhat different from HEL and GS. No stipulation is made for ASD and ASE because of their inconsistent performance. In all cases, the peak factor evaluation based on Vanmarcke's formulation was inappropriate for implementation of these methods, because the values thus obtained were rather high.

7. As mentioned earlier, relative velocity and absolute acceleration response prediction is more error prone if the approximate methods are used. The reason for this can be appreciated if we look at the inelastic response spectra shown in fig. 11 and 13. The enveloping effect in the response spectra for the intermediate frequency is almost non-existent for larger ductility ratios. In fact the curves are of monotonous character for higher ductility values. The elastic spectra are used to determine the response of the equivalent linear system and the readings on these curves are subject to the above mentioned enveloping effect, thus causing a considerable error in the response prediction of these quantities.

8. Considering all the above comments, following recommendations can be made. The approximate methods considered in this work are satisfactory for low to moderate ductilities, particularly for values of α greater than 0.20. Incorporation of a non-zero mean response assumption would probably yield better results in

light of the fact that the actual response is far from the zero mean case when the ductility ratio is high. Also, the methods considered in this study would probably be more satisfactory for modelling the hysteretic response of a multi-degree of freedom system, since modelling the effective stiffness and damping coefficient is more appropriate in such cases.

REFERENCES

1. ASCE-Manuals and Reports on Engineering Practice-No.41, 'Plastic Design in Steel, A Guide and Commentary', Chapter 5 in the Second Edition, ASCE Publication, 1971.

2. Baber, T. T. and Wen, Y. K., 'Equivalent Linearization for Hysteretic Structures', Proceedings of the ASCE Engineering Mechanics Division Specialty Conference on Probabilistic Mechanics and Structural Reliability, Tucson, Arizona, pp. 25-29, January 1979.

3. Baber, T. T. and Wen, Y. K., 'Stochastic Equivalent Linearization for Hysteretic, Degrading, Multistory Structures', A Report submitted to the National Science Foundation, Research Grant No. ENV 77-09090, December 1979.

4. Berg, G. V., 'A Study of Earthquake Response of Inelastic Systems', Proceedings of the 34th convention of the Structural Engineers Association of California, Coronado, CA, pp. 63-67, October 1965.

5. Bouc, R., 'Forced Vibration of Mechanical Systems with Hysteresis', Abstract, Proceedings of the Fourth Conference on Nonlinear Oscillation, Prague, Czechoslovakia, 1967.

6. Caughey, T. K., 'Random Excitation of a System with Bilinear Hysteresis', Journal of Applied Mechanics, Transactions of the ASME, December 1960.

7. Caughey, T. K., 'Nonlinear Theory of Random Vibrations', Advances in Applied Mechanics, Vol. 11, pp. 209-253, 1971.

8. Caughey, T. K., 'Equivalent Linearization Techniques', The Journal of the Acoustical Society of America, No. 35(11), pp. 1706-1711, November 1963.

9. Caughey, T. K., 'Sinusoidal Excitation of a System with Bilinear Hysteresis', Journal of Applied Mechanics, ASME, Vol. 27, No. 4, pp. 649-652, December 1960.

10. Chopra, A. K. and Lopez, O. A., 'Evaluation of Simulated Ground Motions for Predicting Elastic Response of Long Period Structures and Inelastic Response of Structures', Earthquake Engineering and Structural Dynamics, Vol. 7, pp. 383-402, January 1979.

11. Crandall, S. H., 'Perturbation Techniques for Random Vibration of Nonlinear Systems', The Journal of the Acoustical Society of America, Vol. 35, No. 11, November 1963.

12. Gates, N. C., 'The Earthquake Response of Deteriorating Systems', Doctoral Dissertation at California Institute of Technology, Pasadena, CA, March 1977.

13. Grossmayer, R. L., 'Elastic-Plastic Oscillators under Random Excitation', Journal of Sound and Vibration, No. 65(3), pp. 353-379, March 1979.

14. Grossmayer,. R. L., and Iwan, W. D., 'A Linearization Scheme for Hysteretic Systems Subjected to Random Excitation', Earthquake Engineering and Structural Dynamics, Vol. 9, pp. 171-185, 1981.

15. Iwan, W. D. and Patula, E. J., 'The Merit of Different Error Minimization Criteria in Approximate Analysis', Journal of Applied Mechanics, Transactions of ASME, Vol. 39, pp. 257-262, March 1972.

16. Iwan, W. D., 'A generalization of the Concept of Equivalent Linearization', International Journal of Nonlinear Mechanics, Vol. 8, pp. 279-287, 1973.

17. Iwan, W. D. and Gates, N. C., 'Estimating Earthquake Response of Simple Hysteretic Structures', Journal of the Engineering Mechanics Division, ASCE, No. EM3, pp. 391-405, June 1979.

18. Iwan, W. D., 'Estimating Inelastic Response Spectra from Elastic Spectra', Earthquake Engineering and Structural Dynamics, Vol. 8, pp. 375-388, February 1980.

19. Iwan, W. D. and Gates, N. C., 'The Effective Period and Damping of a Class of Hysteretic Structures', Earthquake Engineering and Structural Dynamics, Vol. 7, pp. 199-211, July 1978.

20. Jacobsen, L. S., 'Steady Forced Vibrations as Influenced by Damping', Transactions of ASME, Vol. 51, 1930.

21. Jennings, P. C., Housner, G. W. and Tsai, N. C., 'Simulated Earthquake Motions', Earthquake Engineering Research Lab., California Institute of Technology, Pasadena, CA, April 1968.

22. Jennings, P.. C., 'Equivalent Viscous Damping for Yielding Structures', Journal of the Engineering Mechanics Division, ASCE, Vol. 94, No. EM1, pp. 103-116, February 1968.

23. Lutes, L. D., 'Equivalent Linearization for Random Vibration', Journal of the Engineering Mechanics Division, ASCE, No. EM3, June 1970.

24. Lutes, L. D., ' Approximate Technique for Treating Random Vibration of Hysteretic Systems', The Journal of the Acoustical Society of America, Vol. 48, No. 1(part 2), 1970.

25. Nau, J. M., 'Computation of Inelastic Response Spectra', Journal of the Engineering Mechanics Division, ASCE, Vol. 109, No. 1, February 1983.

26. Newmark, N. M., Blume, J. A. and Kapoor, K. K., 'Seismic Design Spectra for Nuclear Power Plants', Journal of the Power Division, ASCE, Vol. 99, 1973.

27. Newmark, N. M., 'A Method of Computation for Structural Dynamics', Transactions, ASCE, Vol. 127, pp. 1406-1435, 1962.

28. Newmark N. M. and Hall, W. J., 'Procedures and Criteria for Earthquake-Resistant Design', Building Practices for Disaster Mitigation, Building Science Series 46, NBS, pp. 209-237, 1973.

29. Newmark, N. M. and Rosenblueth, E., Fundamentals of Earthquake Engineering, Prentice Hall, Inc., Englewood Cliffs, New Jersey, 1971.

30. Nigam, N. C. and Jennings, P. C., 'Calculation of Response Spectra from Strong-Motion Earthquake Records', Bulletin of the Seismological Society of America, Vol. 59, No. 2, April 1969.

31. Nigam, N. C. and Jennings, P. C., 'Digital Calculation of Response Spectra from Strong-Motion Earthquake Records', Earthquake Engineering Research Lab., California Institute of Technology, Pasadena, CA, June 1968.

32. Paz, M., 'Structural Dynamics, Theory and Computation', Chapter 7, Van Nostrand Reinhold Company, New York, 1980.

33. Radoshycka, J. B., 'Dynamic Response of Single-Degree-of-Freedom Bilinear Systems', M.S. Thesis, Rice University, May 1966.

34. Ramberg, W. and Osgood, W. T., ' Description of Stress-Strain Curves by Three Parameters', Technical Note 902, National Advisory Committee for Aeronautics, 1943.

35. Rice, S. O., 'Mathematical Analysis of Random Noise', in Selected Papers on Noise an Stochastic Processes, Ed. N. Wax, Dover Publications, Inc., New York, 1954.

36. Riddell, R., 'Statistical Analysis of the Response of Nonlinear Systems Subjected to Earthquakes', Doctoral Dissertation, University of Illinois, Urbana, Illinois, August 1979.

37. Rosenblueth, E. and Herrera, I., 'On a Kind of Hysteresis Damping', Journal of the Engineering Mechanics Division, ASCE, Vol. 90, No. EM4, pp. 37-48, August 1964.

38. Sharma, A. M. and Singh, M. P., 'Direct Generation of Seismic Floor Response Spectra for Classically and Non-Classically Damped Structures', Technical Report No. VPI-E-83-44, College of Engineering, VPI&SU, November 1983.

39. Singh, M. P. and Ashtiany M. G., 'Seismic Stability Evaluation of Earth Structures', Technical Report No. VPI-E-80.30, College of Engineering, VPI&SU, November 1980.

40. Singh, M. P. and Khatua, T. P., 'Stochastic Seismic Stability Prediction of Earth Dams', Proceedings of the Specialty Conference in Earthquake Engineering and Soil Dynamics, Pasadena, CA, June 1978.

41. Spanos, P-T. D., 'Hysteretic Structural Vibrations under Random Load', The Journal of the Acoustical Society of America, Vol. 65, No. 2, pp. 404-410, February 1979.

42. Tsai, N. C., 'Spectrum Compatible Motions for Design Purposes', Journal of the Engineering Mechanics Division, ASCE, April 1972.

43. Vanmarcke, E. H., 'Seismic Structural Response', Chapter 8 in Seismic Risk and Engineering Decisions, Ed. C. Lomnitz and E. Rosenbleuth, Elsevier Scientific Publishing Company, New York, 1976.

44. Vanmarcke, E. H. and Gasparini, D. A., 'Simulated Earthquake Ground Motions', Transactions of the Fourth SMiRT Conference, Paper K1/9, Vol. K(a), San Fransico, CA, August 1977.

45. Wen, Y. K., 'Method for Random Vibration of Hysteretic Systems', Journal of the Engineering Mechanics Division, ASCE, No. EM4, April 1976.

46. Wen, Y. K., 'Equivalent linearization for Hysteretic Systems under Random Excitation', Journal of Applied Mechanics, Transactions of the ASME, Vol. 47, March 1980.

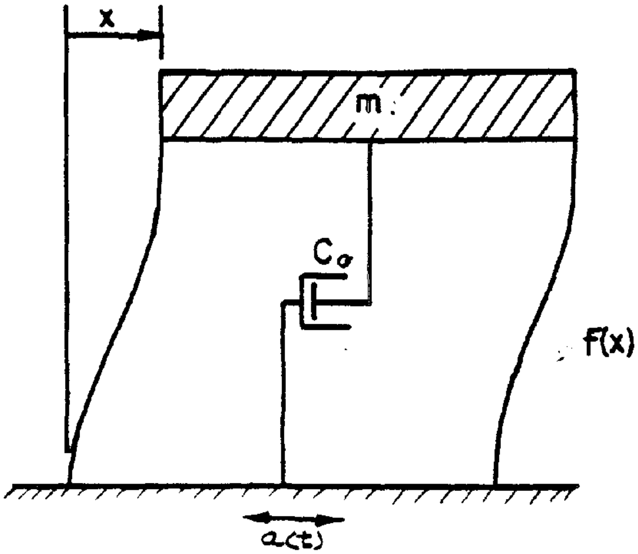

Fig. 1(a) Shear Beam Model Representation of One Story Structure (SDOF System)

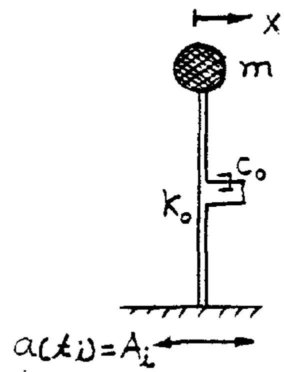

Fig. 1(b) SDOF Oscillator

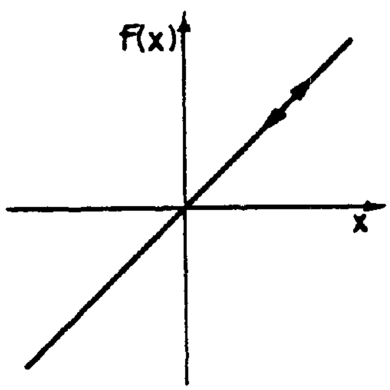

Fig. 2 Linear Elastic Behavior

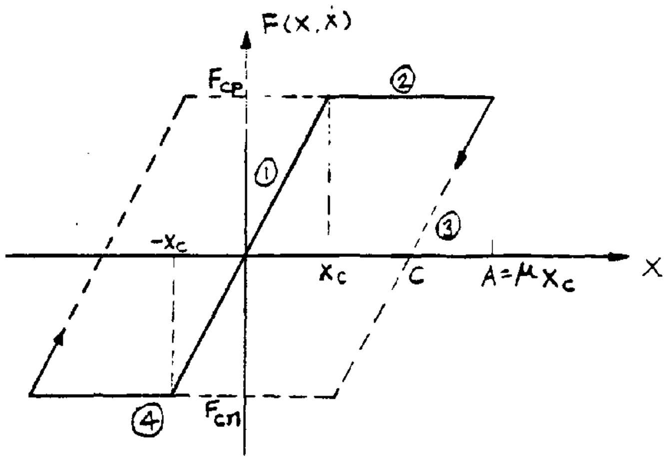

Fig. 3 Elasto-Plastic Behavior

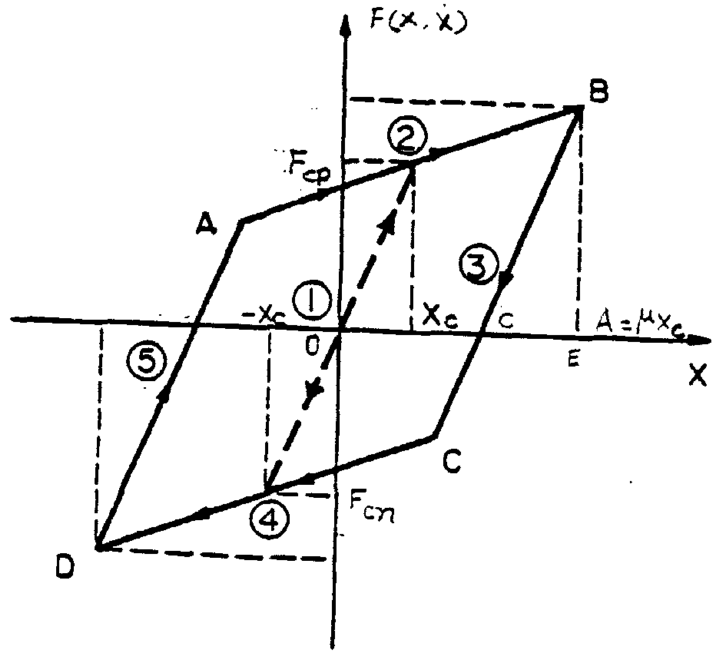

Fig. 4 Bilinear Hysteretic (BLH) Behavior

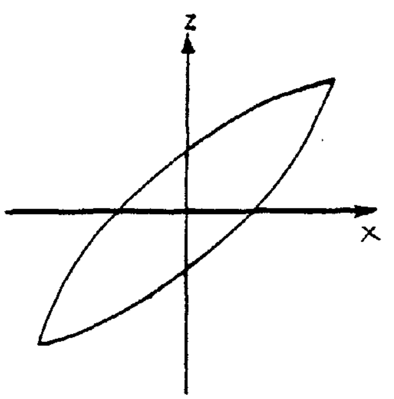

Fig. 5(a) Representation of the Hysteretic Force Component in WBB Oscillator

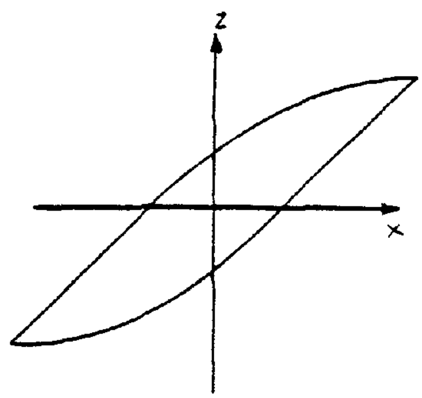

Fig. 5(b) Representation of the Hysteretic Force Component in WBB Oscillator

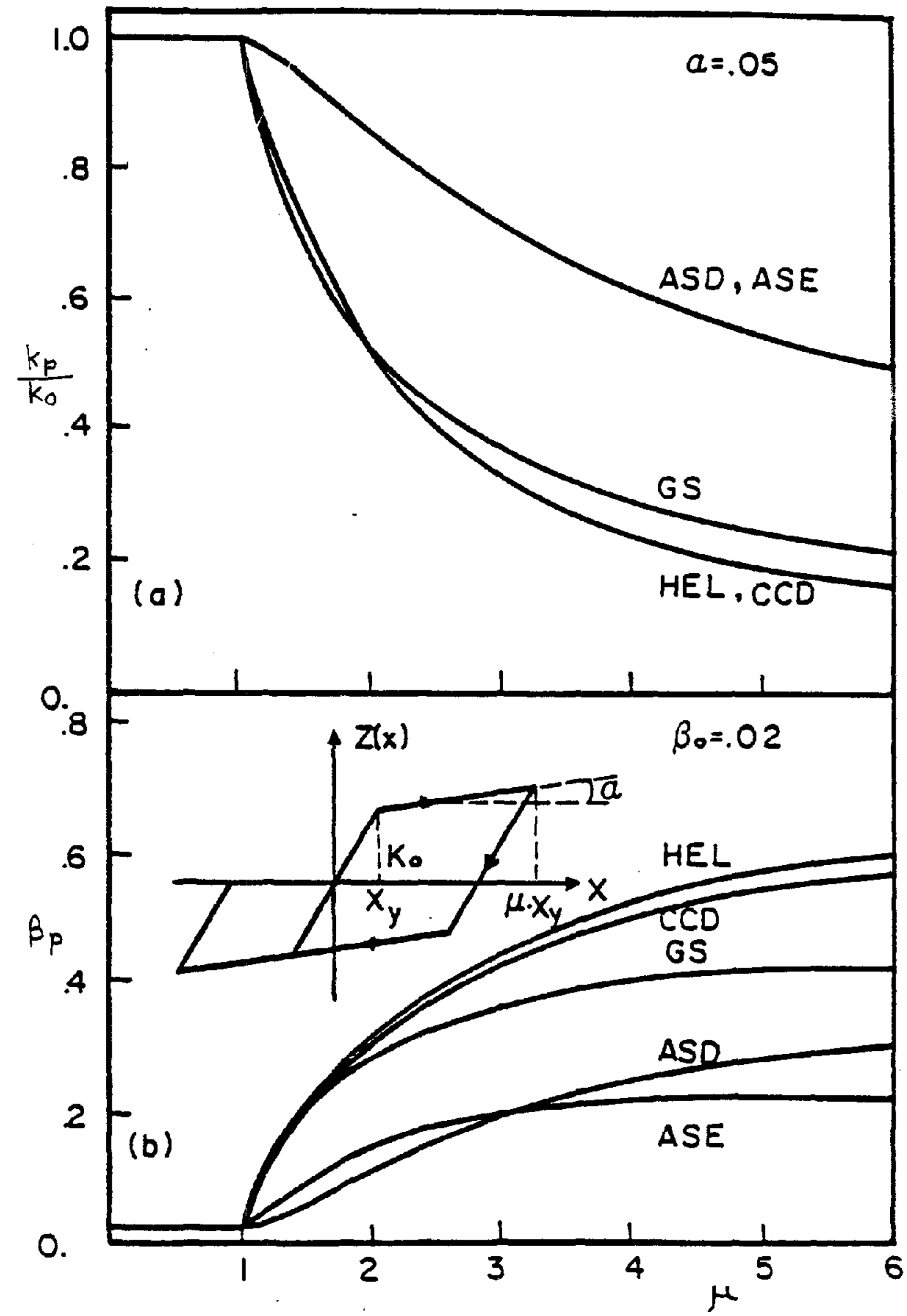

Fig. 6 Effective Non-Hysteretic Properties Given by Various Methods

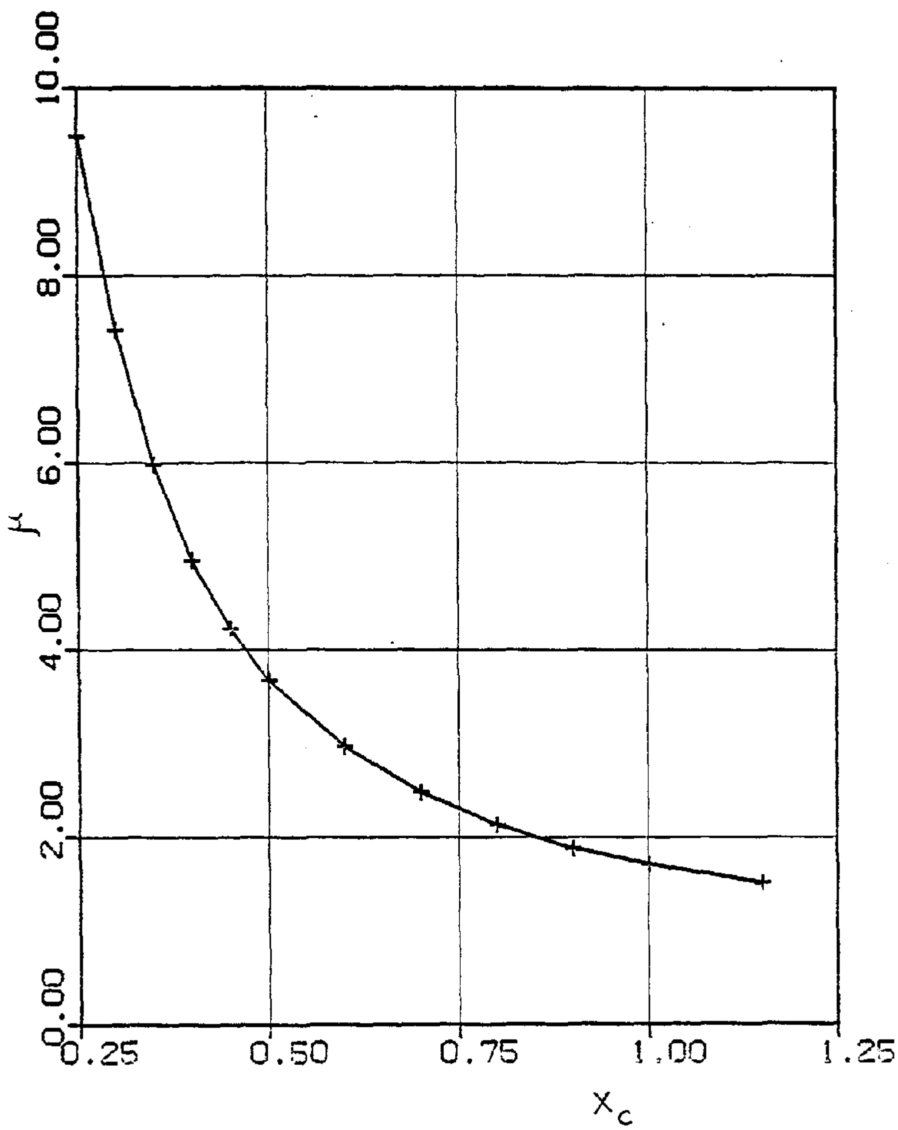

Fig. 7 Yield Displacement Versus Ductility for α = 0, β_0 = .05 and 1 cps Natural Frequency

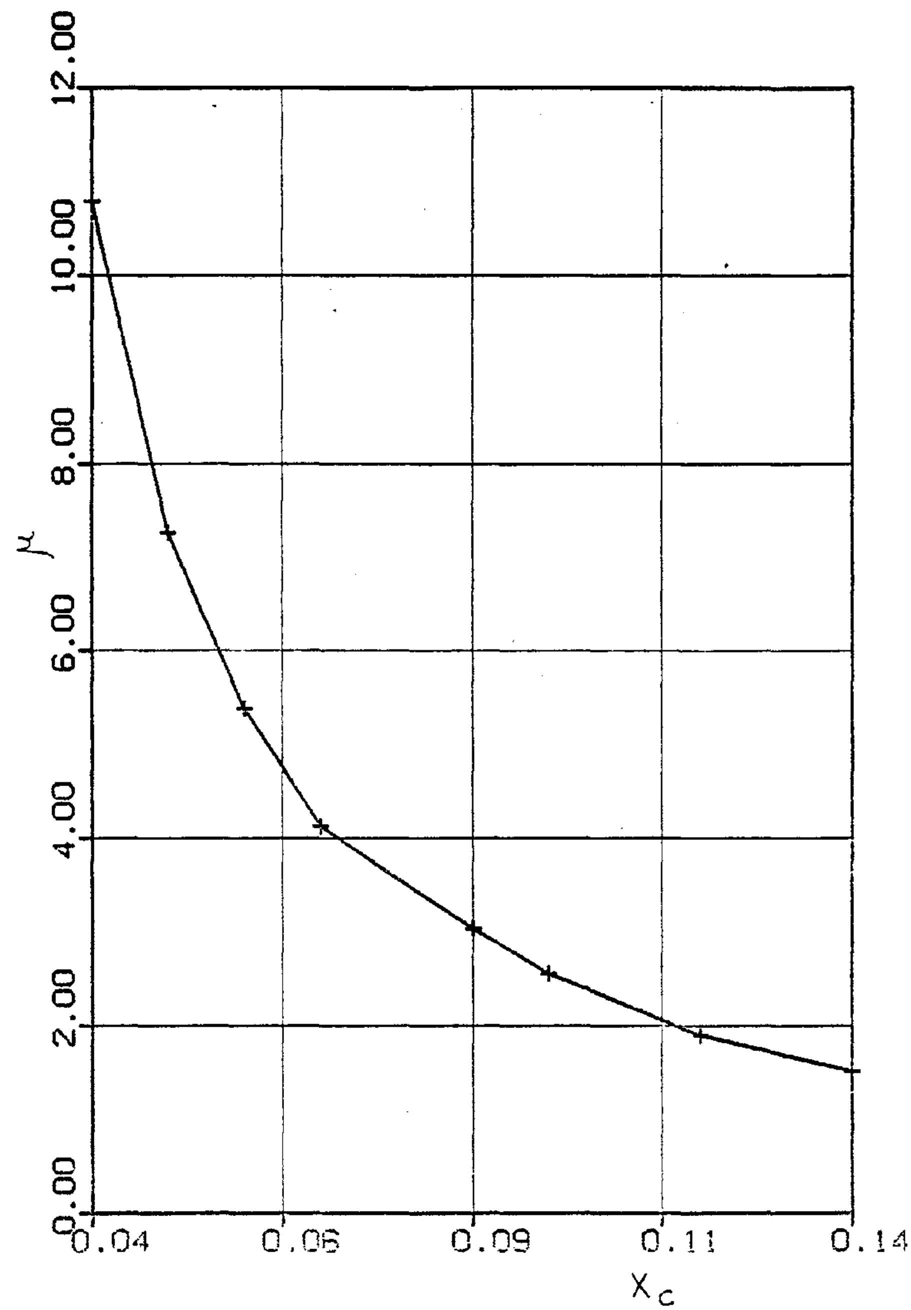

Fig. 8 Yield Displacement Versus Ductility for $\alpha = 0$, $\beta_o = .05$ and 5 cps Natural Frequency

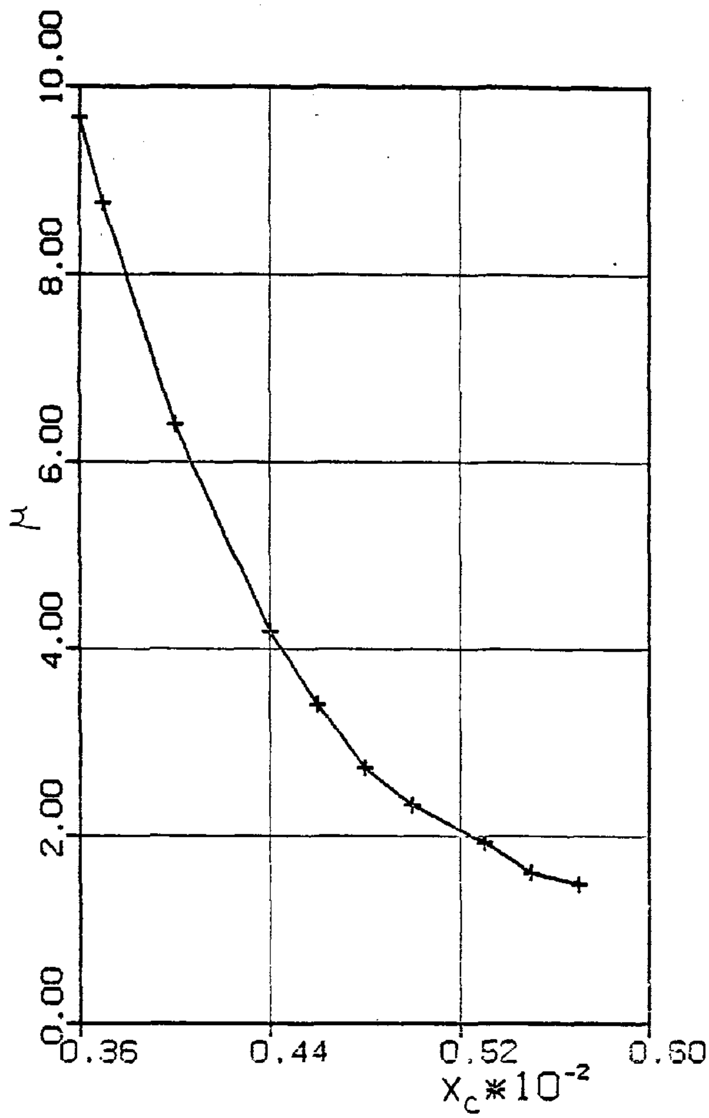

Fig. 9 Yield Displacement Versus Ductility for $\alpha = 0$, $\beta_0 = .05$ and 20 cps Natural Frequency

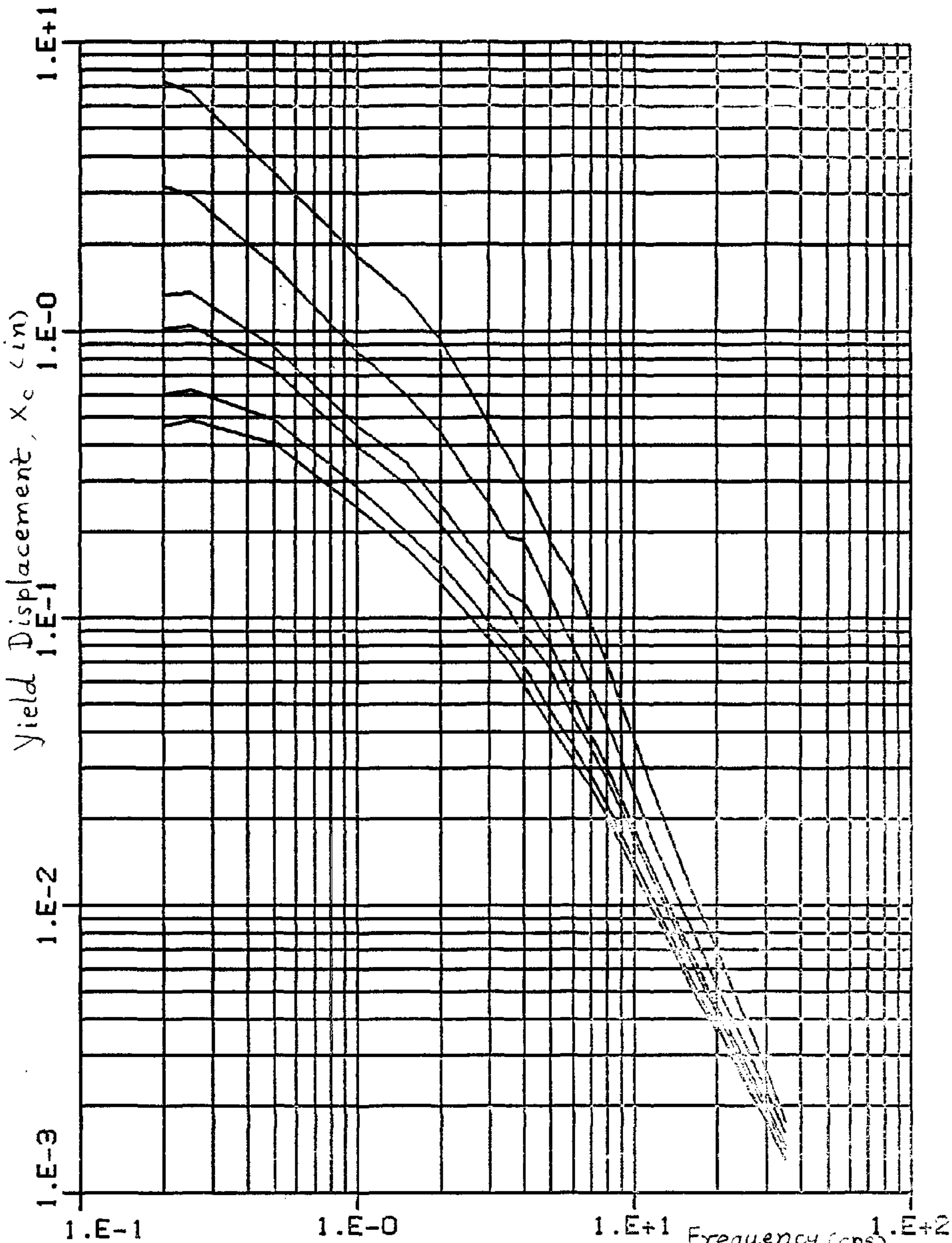

Fig. 10 Response Spectrum for Relative Displacement (α = 0, β_0 = .05)

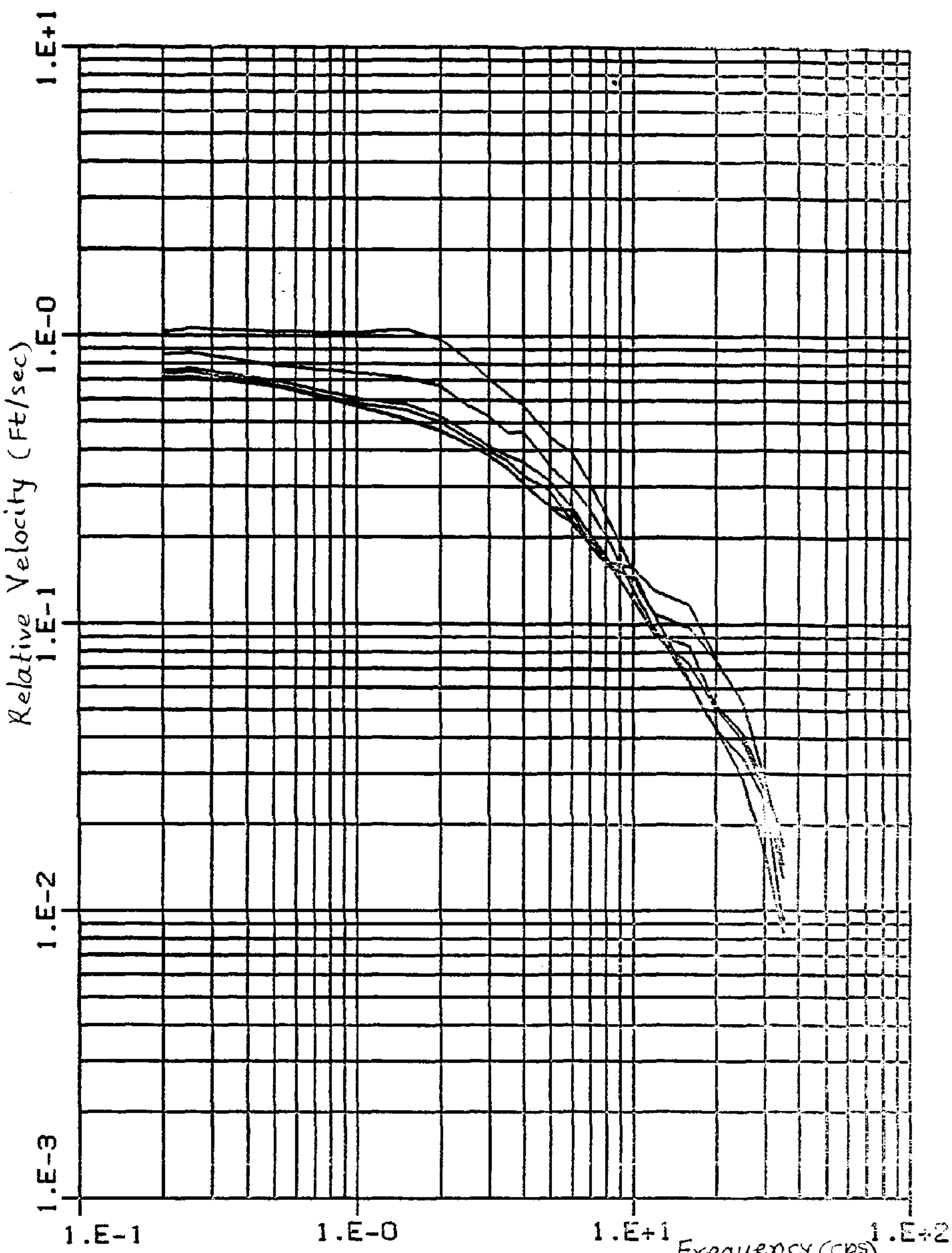

Fig. 11 Response Spectrum for Relative Velocity (α = 0, β_0 = .05)

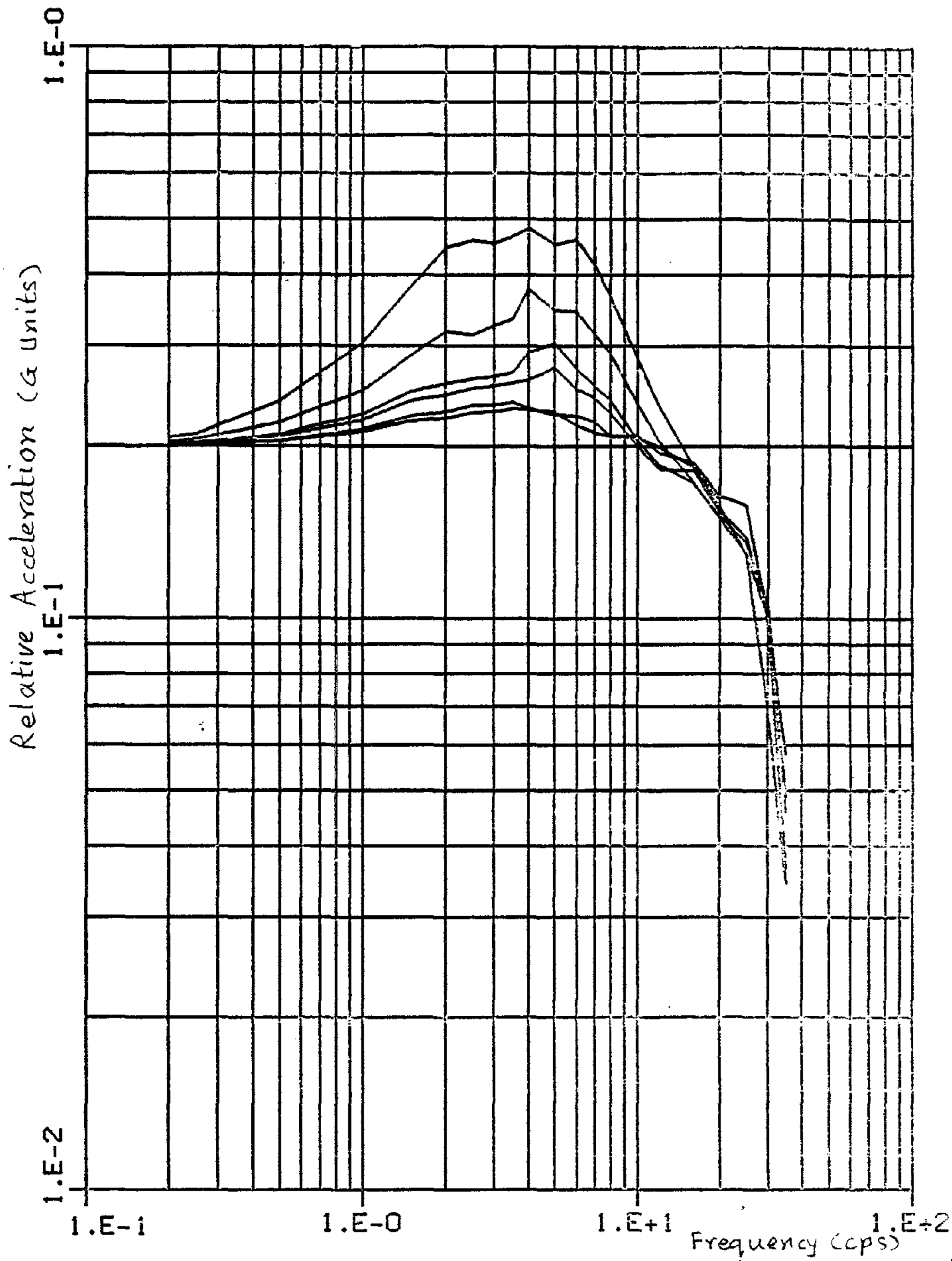

Fig. 12 Response Spectrum for Relative Acceleration (α = 0, β_0 = .05)

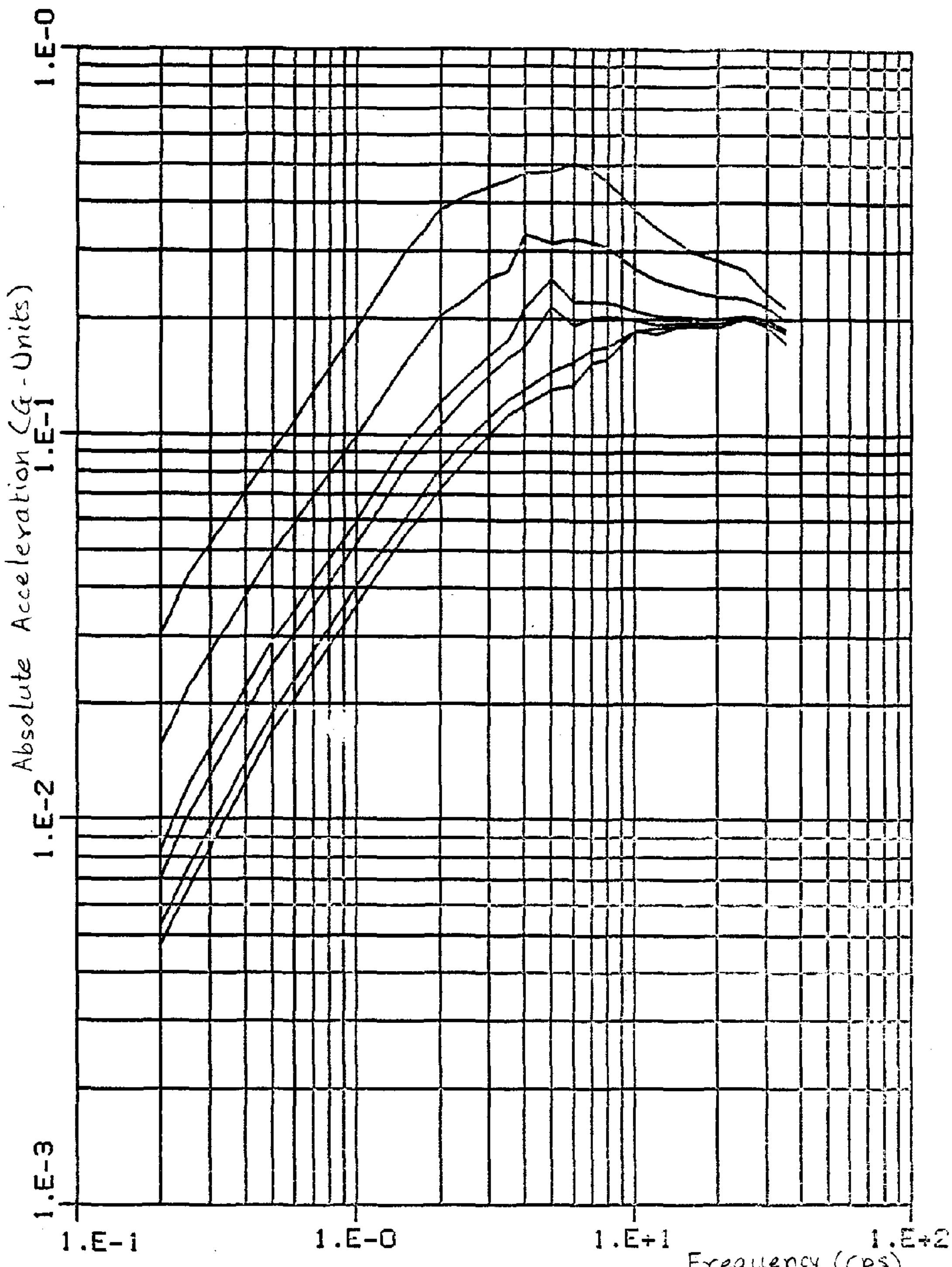

Fig. 13 Response Spectrum for Absolute Acceleration (α = 0, β_0 = .05)

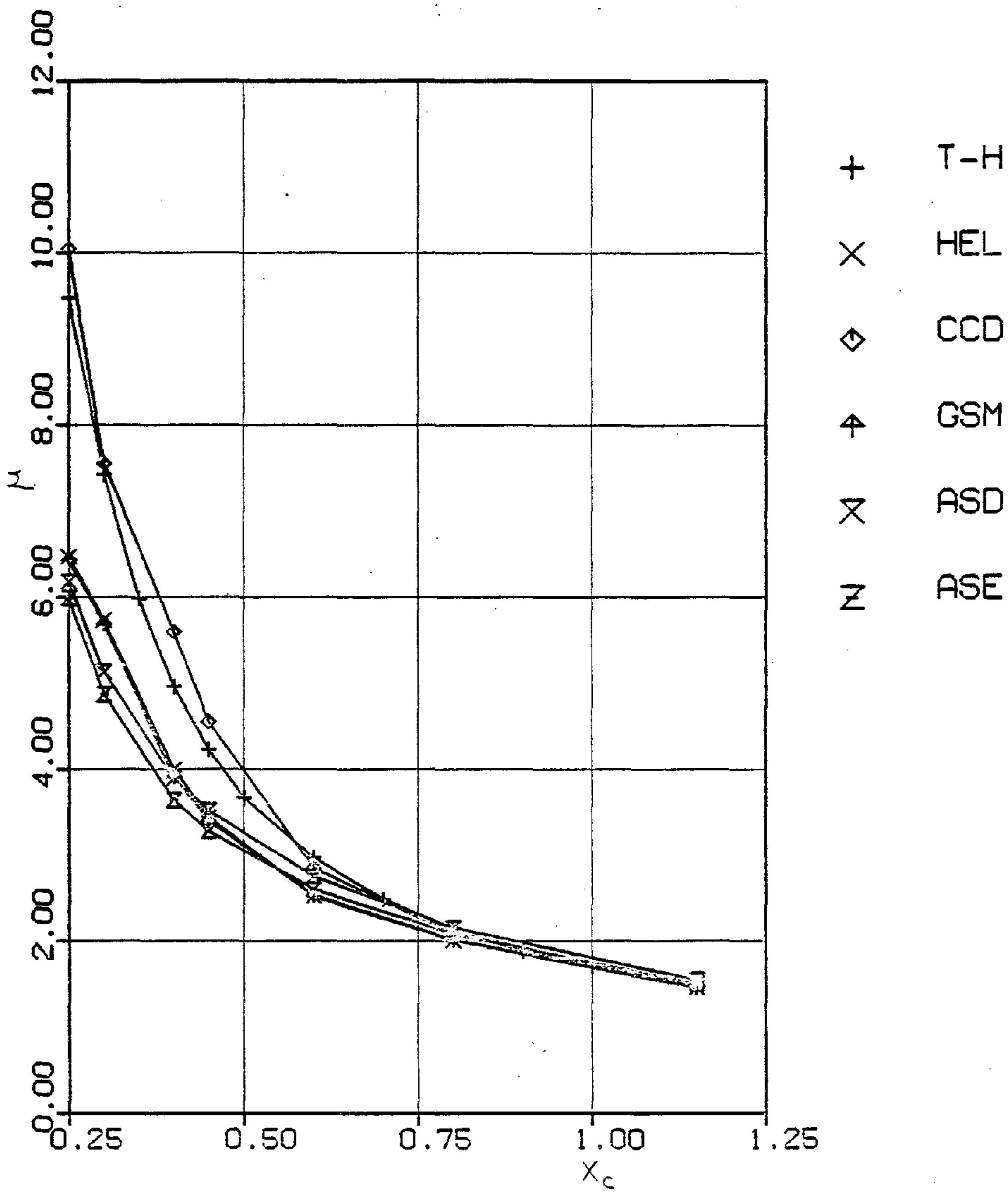

Fig. 14 Prediction of Ductility Using Various Methods for α = 0, β_0 = .05 and f = 1 cps (Assumed μ_f = 2.00)

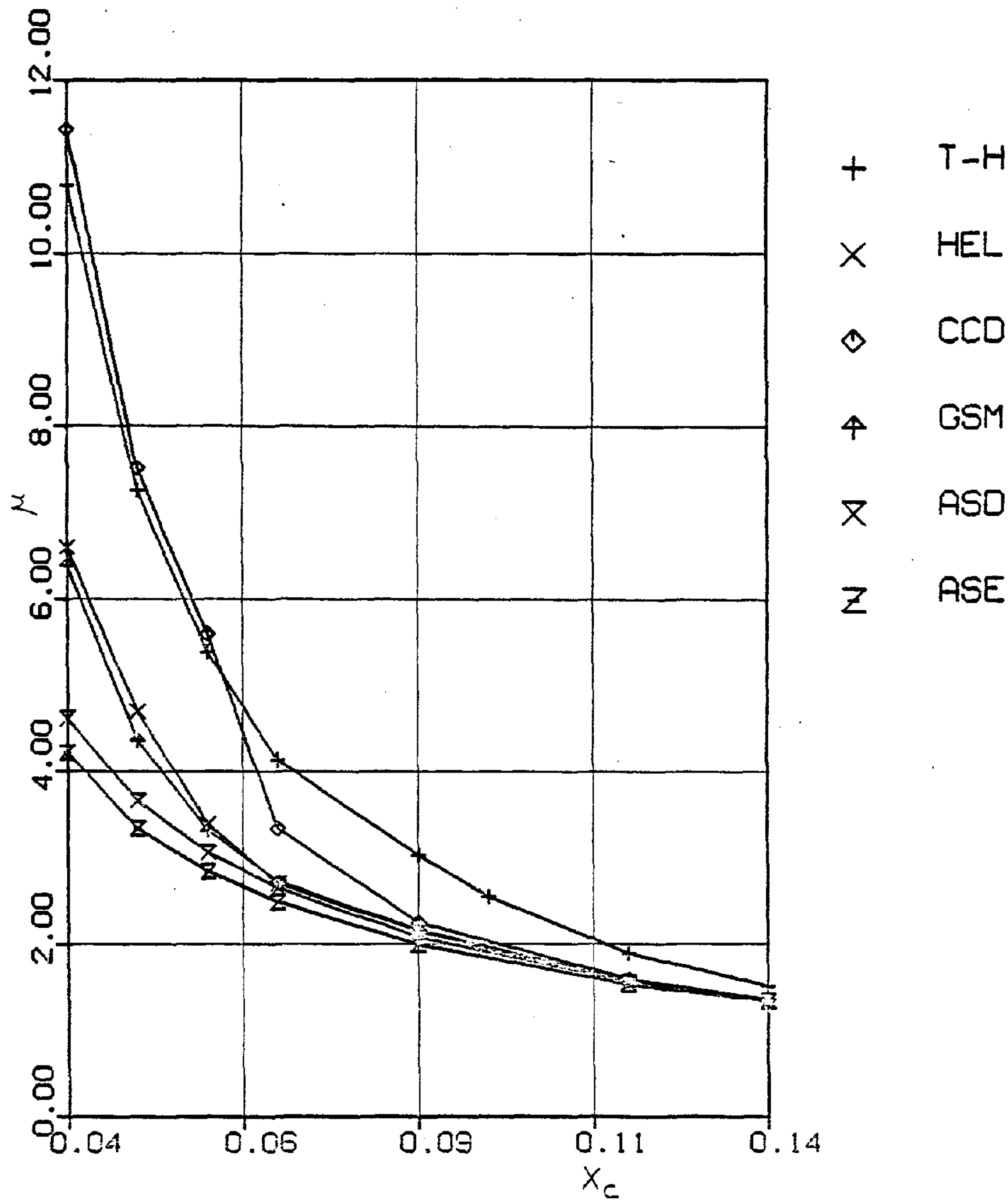

Fig. 15 Prediction of Ductility Using Various Methods for $\alpha = 0$, $\beta_0 = .05$ and f = 5 cps (Assumed $\mu_f = 2.20$)

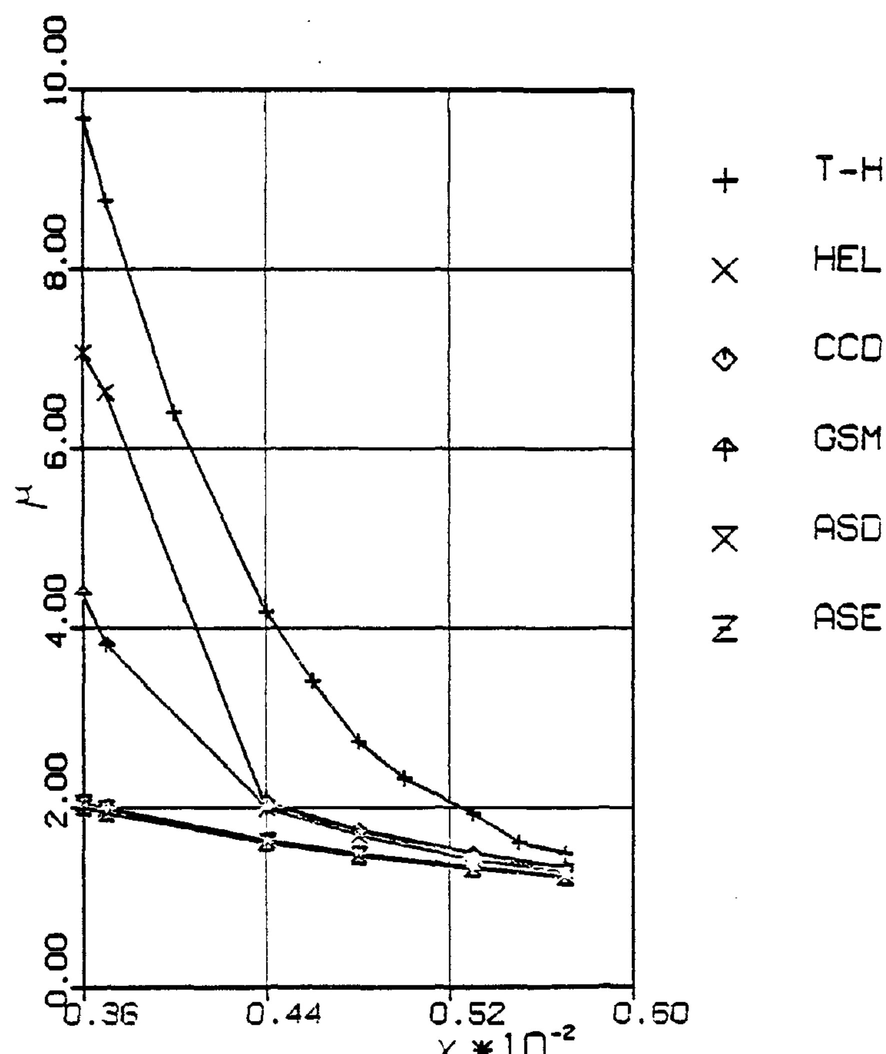

Fig. 16 Prediction of Ductility Using Various Methods for $\alpha = 0$, $\beta_0 = .05$ and f = 20 cps (Assumed Pf = 210)

Table 1

Parameters of Spectral Density Function

$\Phi_g(\omega)$, Eq. (4.2)

i	δ_i ft^2-sec/rad	ω_i rad/sec	β_i
1	.0015	13.50	.3925
2	.000495	23.50	.3600
3	.000375	39.00	.3350

Table 2

Values of Natural Frequency (cps) Considered for

Generation of the Inelastic Response Spectra

.20	.25	.50	1.00	1.50	2.00	2.50	3.00	3.50
4.0	5.0	6.0	7.0	8.0	10.0	12.0	16.0	20.0
25.0	30.0	35.0						

Table 3 Comparison of Response Prediction Using Various Methods

NATURAL FREQUENCY OF THE OSCILLATOR = 1.00
DAMPING RATIO FOR THE SYSTEM = 0.05
RATIO OF THE TWO SPRING STIFFNESSES = 0.00

RESPONSE FOR YIELD DISPLACEMENT = 0.8000

RESULTS OF TIME-HISTORY ANALYSIS

MEAN DUCTILITY RATIO = 2.1280
MEAN PEAK FACTOR (ON DISPLACEMENT) = 1.7360
AVERAGE MAXIMUM RELATIVE VELOCITY = 0.726483
AVERAGE MAXIMUM RELATIVE ACCELERATION = 0.224716
AVERAGE MAXIMUM ABSOLUTE ACCELERATION = 0.093641

RESULTS OF THE EQUIVALENT LINEAR ANALYSES

METHOD	PFC	PERIOD	DAMPING	DRC	RSVC	RSAC	ASAC
HEL	2.000	1.1909	0.10941	2.0076	0.797357	0.249924	0.119693
GSM	2.000	1.2013	0.11107	2.0109	0.793536	0.248596	0.117965
CCD	2.000	1.2092	0.10284	2.0842	0.812685	0.250609	0.119912
ASD	2.000	1.0597	0.06721	2.1532	0.924967	0.281064	0.158981
ASE	2.000	1.0548	0.07455	2.0767	0.899135	0.277688	0.155185

Table 4 Comparison of Response Prediction Using Various Methods

NATURAL FREQUENCY OF THE OSCILLATOR = 1.00
DAMPING RATIO FOR THE SYSTEM = 0.05
RATIO OF THE TWO SPRING STIFFNESSES = 0.00

RESPONSE FOR YIELD DISPLACEMENT = 0.4000

RESULTS OF TIME-HISTORY ANALYSIS

MEAN DUCTILITY RATIO = 4.9565
MEAN PEAK FACTOR (ON DISPLACEMENT) = 1.5410
AVERAGE MAXIMUM RELATIVE VELOCITY = 0.584925
AVERAGE MAXIMUM RELATIVE ACCELERATION = 0.222420
AVERAGE MAXIMUM ABSOLUTE ACCELERATION = 0.052040

RESULTS OF THE EQUIVALENT LINEAR ANALYSES

METHOD	PFC	PERIOD	DAMPING	DRC	RSVC	RSAC	ASAC
HEL	1.700	1.8993	0.32919	4.1838	0.600443	0.210840	0.064251
GSM	1.700	1.7548	0.28814	4.1118	0.624383	0.214000	0.068972
CCD	2.200	1.8611	0.19373	5.2120	0.723054	0.220556	0.069317

Table 5 Comparison of Response Prediction Using Various Methods

NATURAL FREQUENCY OF THE OSCILLATOR = 1.00
DAMPING RATIO FOR THE SYSTEM = 0.05
RATIO OF THE TWO SPRING STIFFNESSES = 0.00

RESPONSE FOR YIELD DISPLACEMENT = 0.3000

RESULTS OF TIME-HISTORY ANALYSIS

MEAN DUCTILITY RATIO = 7.4212
MEAN PEAK FACTOR (ON DISPLACEMENT) = 1.5950
AVERAGE MAXIMUM RELATIVE VELOCITY = 0.571108
AVERAGE MAXIMUM RELATIVE ACCELERATION = 0.215531
AVERAGE MAXIMUM ABSOLUTE ACCELERATION = 0.041726

RESULTS OF THE EQUIVALENT LINEAR ANALYSES

METHOD	PFC	PERIOD	DAMPING	DRC	RSVC	RSAC	ASAC
HEL	2.000	2.0561	0.36232	5.7278	0.586604	0.208668	0.060071
GSM	2.000	1.8721	0.30670	5.6944	0.614332	0.212232	0.064924
CCD	2.200	2.2648	0.25659	7.4268	0.672660	0.213729	0.055785

Table 6 Comparison of Response Prediction Using Various Methods

NATURAL FREQUENCY OF THE OSCILLATOR = 5.00
DAMPING RATIO FOR THE SYSTEM = 0.05
RATIO OF THE TWO SPRING STIFFNESSES = 0.00

RESPONSE FOR YIELD DISPLACEMENT = 0.1200

RESULTS OF TIME-HISTORY ANALYSIS

MEAN DUCTILITY RATIO = 1.8882
MEAN PEAK FACTOR (ON DISPLACEMENT) = 1.4490
AVERAGE MAXIMUM RELATIVE VELOCITY = 0.367780
AVERAGE MAXIMUM RELATIVE ACCELERATION = 0.358980
AVERAGE MAXIMUM ABSOLUTE ACCELERATION = 0.333450

RESULTS OF THE EQUIVALENT LINEAR ANALYSES

METHOD	PFC	PERIOD	DAMPING	DRC	RSVC	RSAC	ASAC
HEL	1.600	0.2376	0.10772	1.5968	0.389493	0.345792	0.353902
GSM	1.600	0.2402	0.11103	1.6085	0.388232	0.342111	0.349351
CCD	1.800	0.2343	0.08428	1.7225	0.429448	0.382572	0.390226

Table 7 Comparison of Response Prediction Using Various Methods

NATURAL FREQUENCY OF THE OSCILLATOR = 5.00
DAMPING RATIO FOR THE SYSTEM = 0.05
RATIO OF THE TWO SPRING STIFFNESSES = 0.00

RESPONSE FOR YIELD DISPLACEMENT = 0.0700

RESULTS OF TIME-HISTORY ANALYSIS

MEAN DUCTILITY RATIO = 4.1294
MEAN PEAK FACTOR (ON DISPLACEMENT) = 1.3480
AVERAGE MAXIMUM RELATIVE VELOCITY = 0.283860
AVERAGE MAXIMUM RELATIVE ACCELERATION = 0.269730
AVERAGE MAXIMUM ABSOLUTE ACCELERATION = 0.205140

RESULTS OF THE EQUIVALENT LINEAR ANALYSES

METHOD	PFC	PERIOD	DAMPING	DRC	RSVC	RSAC	ASAC
HEL	1.600	0.3448	0.28855	3.2902	0.321648	0.228853	0.225130
GSM	1.600	0.3194	0.25590	3.0785	0.320487	0.238440	0.240590
CCD	2.000	0.3440	0.18436	4.0949	0.407676	0.276790	0.262361

Table 8 Comparison of Response Prediction Using Various Methods

NATURAL FREQUENCY OF THE OSCILLATOR = 5.00
DAMPING RATIO FOR THE SYSTEM = 0.05
RATIO OF THE TWO SPRING STIFFNESSES = 0.00

RESPONSE FOR YIELD DISPLACEMENT = 0.0500

RESULTS OF TIME-HISTORY ANALYSIS

MEAN DUCTILITY RATIO = 7.2582
MEAN PEAK FACTOR (ON DISPLACEMENT) = 1.3350
AVERAGE MAXIMUM RELATIVE VELOCITY = 0.253790
AVERAGE MAXIMUM RELATIVE ACCELERATION = 0.234360
AVERAGE MAXIMUM ABSOLUTE ACCELERATION = 0.152180

RESULTS OF THE EQUIVALENT LINEAR ANALYSES

METHOD	PFC	PERIOD	DAMPING	DRC	RSVC	RSAC	ASAC
HEL	1.800	0.4180	0.38531	5.3143	0.316405	0.211158	0.194068
GSM	1.800	0.3732	0.30580	5.0808	0.332450	0.227027	0.215066
CCD	2.200	0.4566	0.26024	7.5231	0.422536	0.250740	0.208918

Table 9 Comparison of Response Prediction Using Various Methods

NATURAL FREQUENCY OF THE OSCILLATOR = 16.00
DAMPING RATIO FOR THE SYSTEM = 0.05
RATIO OF THE TWO SPRING STIFFNESSES = 0.00

RESPONSE FOR YIELD DISPLACEMENT = 0.0080

RESULTS OF TIME-HISTORY ANALYSIS

MEAN DUCTILITY RATIO = 2.3454
MEAN PEAK FACTOR (ON DISPLACEMENT) = 1.3280
AVERAGE MAXIMUM RELATIVE VELOCITY = 0.063080
AVERAGE MAXIMUM RELATIVE ACCELERATION = 0.171680
AVERAGE MAXIMUM ABSOLUTE ACCELERATION = 0.225850

RESULTS OF THE EQUIVALENT LINEAR ANALYSES

METHOD	PFC	PERIOD	DAMPING	DRC	RSVC	RSAC	ASAC
HEL	1.800	0.0759	0.12332	1.8971	0.061075	0.141499	0.272211
GSM	1.700	0.0861	0.19099	2.3219	0.064339	0.128311	0.262637
CCD	1.900	0.0744	0.09487	1.9068	0.065635	0.158271	0.283605

Table 10 Comparison of Response Prediction Using Various Methods

NATURAL FREQUENCY OF THE OSCILLATOR = 16.00
DAMPING RATIO FOR THE SYSTEM = 0.05
RATIO OF THE TWO SPRING STIFFNESSES = 0.00

RESPONSE FOR YIELD DISPLACEMENT = 0.0070

RESULTS OF TIME-HISTORY ANALYSIS

MEAN DUCTILITY RATIO = 3.8253
MEAN PEAK FACTOR (ON DISPLACEMENT) = 1.2360
AVERAGE MAXIMUM RELATIVE VELOCITY = 0.070620
AVERAGE MAXIMUM RELATIVE ACCELERATION = 0.171240
AVERAGE MAXIMUM ABSOLUTE ACCELERATION = 0.203610

RESULTS OF THE EQUIVALENT LINEAR ANALYSES

METHOD	PFC	PERIOD	DAMPING	DRC	RSVC	RSAC	ASAC
HEL	1.850	ITERATION LIMIT EXCEEDED					
GSM	1.750	0.1044	0.27196	3.7476	0.078404	0.128222	0.260438
CCD	1.950	ITERATION LIMIT EXCEEDED					

Table 11 Comparison of Response Prediction Using Various Methods

NATURAL FREQUENCY OF THE OSCILLATOR = 1.50
DAMPING RATIO FOR THE SYSTEM = 0.10
RATIO OF THE TWO SPRING STIFFNESSES = 0.25

RESPONSE FOR YIELD DISPLACEMENT = 0.3000

RESULTS OF TIME-HISTORY ANALYSIS

MEAN DUCTILITY RATIO = 3.0765
MEAN PEAK FACTOR (ON DISPLACEMENT) = 1.9740
AVERAGE MAXIMUM RELATIVE VELOCITY = 0.563260
AVERAGE MAXIMUM RELATIVE ACCELERATION = 0.243750
AVERAGE MAXIMUM ABSOLUTE ACCELERATION = 0.115170

RESULTS OF THE EQUIVALENT LINEAR ANALYSES

METHOD	PFC	PERIOD	DAMPING	DRC	RSVC	RSAC	ASAC
HEL	1.600	0.9194	0.23642	3.0340	0.584265	0.239256	0.126590
GSM	1.600	0.8989	0.22986	3.0064	0.589492	0.241786	0.130047
CCD	1.600	0.9558	0.19204	3.4927	0.643067	0.247092	0.128628
ASD	1.600	0.7528	0.15022	3.1245	0.696851	0.277173	0.177720
ASE	1.600	0.7462	0.16566	2.9495	0.665743	0.271013	0.173000

Table 12 Comparison of Response Prediction Using Various Methods

NATURAL FREQUENCY OF THE OSCILLATOR = 1.50
DAMPING RATIO FOR THE SYSTEM = 0.10
RATIO OF THE TWO SPRING STIFFNESSES = 0.25

RESPONSE FOR YIELD DISPLACEMENT = 0.2000

RESULTS OF TIME-HISTORY ANALYSIS

MEAN DUCTILITY RATIO = 4.6974
MEAN PEAK FACTOR (ON DISPLACEMENT) = 1.9020
AVERAGE MAXIMUM RELATIVE VELOCITY = 0.537880
AVERAGE MAXIMUM RELATIVE ACCELERATION = 0.230980
AVERAGE MAXIMUM ABSOLUTE ACCELERATION = 0.098520

RESULTS OF THE EQUIVALENT LINEAR ANALYSES

METHOD	PFC	PERIOD	DAMPING	DRC	RSVC	RSAC	ASAC
HEL	1.600	1.0280	0.27073	4.7520	0.563355	0.228189	0.110680
GSM	1.600	0.9859	0.25329	4.7161	0.574129	0.232806	0.116908
CCD	1.600	1.0555	0.22568	5.3229	0.610624	0.234082	0.111855
ASD	1.600	0.8018	0.17403	4.6103	0.654156	0.262601	0.157628
ASE	1.600	0.7965	0.18650	4.4311	0.633994	0.258707	0.154991

Table 13 Comparison of Response Prediction Using Various Methods

NATURAL FREQUENCY OF THE OSCILLATOR = 6.00
DAMPING RATIO FOR THE SYSTEM = 0.10
RATIO OF THE TWO SPRING STIFFNESSES = 0.25

RESPONSE FOR YIELD DISPLACEMENT = 0.0550

RESULTS OF TIME-HISTORY ANALYSIS

MEAN DUCTILITY RATIO = 1.9911
MEAN PEAK FACTOR (ON DISPLACEMENT) = 2.3290
AVERAGE MAXIMUM RELATIVE VELOCITY = 0.227370
AVERAGE MAXIMUM RELATIVE ACCELERATION = 0.259570
AVERAGE MAXIMUM ABSOLUTE ACCELERATION = 0.266050

RESULTS OF THE EQUIVALENT LINEAR ANALYSES

METHOD	PFC	PERIOD	DAMPING	DRC	RSVC	RSAC	ASAC
HEL	1.800	0.1941	0.16467	1.9867	0.251881	0.266856	0.308592
GSM	1.800	0.1959	0.16785	2.0050	0.251575	0.264928	0.306147
CCD	1.800	0.1980	0.15475	2.1185	0.265657	0.276538	0.314789

Table 14 Comparison of Response Prediction Using Various Methods

NATURAL FREQUENCY OF THE OSCILLATOR = 6.00
DAMPING RATIO FOR THE SYSTEM = 0.10
RATIO OF THE TWO SPRING STIFFNESSES = 0.25

RESPONSE FOR YIELD DISPLACEMENT = 0.0320

RESULTS OF TIME-HISTORY ANALYSIS

MEAN DUCTILITY RATIO = 3.9432
MEAN PEAK FACTOR (ON DISPLACEMENT) = 2.4500
AVERAGE MAXIMUM RELATIVE VELOCITY = 0.203070
AVERAGE MAXIMUM RELATIVE ACCELERATION = 0.220870
AVERAGE MAXIMUM ABSOLUTE ACCELERATION = 0.215910

RESULTS OF THE EQUIVALENT LINEAR ANALYSES

METHOD	PFC	PERIOD	DAMPING	DRC	RSVC	RSAC	ASAC
HEL	2.000	0.2345	0.24208	4.0718	0.247400	0.234846	0.264284
GSM	2.000	0.2267	0.23222	3.9048	0.244846	0.236941	0.269166
CCD	2.000	0.2464	0.19393	4.9274	0.294821	0.265974	0.281682

Table 15 Comparison of Response Prediction Using Various Methods

NATURAL FREQUENCY OF THE OSCILLATOR = 20.00
DAMPING RATIO FOR THE SYSTEM = 0.10
RATIO OF THE TWO SPRING STIFFNESSES = 0.25

RESPONSE FOR YIELD DISPLACEMENT = 0.0044

RESULTS OF TIME-HISTORY ANALYSIS

MEAN DUCTILITY RATIO = 1.8579
MEAN PEAK FACTOR (ON DISPLACEMENT) = 2.4300
AVERAGE MAXIMUM RELATIVE VELOCITY = 0.031870
AVERAGE MAXIMUM RELATIVE ACCELERATION = 0.107690
AVERAGE MAXIMUM ABSOLUTE ACCELERATION = 0.222930

RESULTS OF THE EQUIVALENT LINEAR ANALYSES

METHOD	PFC	PERIOD	DAMPING	DRC	RSVC	RSAC	ASAC
HEL	1.600	0.0593	0.17480	1.8687	0.033622	0.095188	0.243056
GSM	1.600	0.0600	0.17970	1.9084	0.033908	0.094740	0.242682
CCD	1.700	0.0576	0.14220	1.8141	0.034980	0.103879	0.248283

Table 16 Comparison of Response Prediction Using Various Methods

NATURAL FREQUENCY OF THE OSCILLATOR = 20.00
DAMPING RATIO FOR THE SYSTEM = 0.10
RATIO OF THE TWO SPRING STIFFNESSES = 0.25

RESPONSE FOR YIELD DISPLACEMENT = 0.0036

RESULTS OF TIME-HISTORY ANALYSIS

MEAN DUCTILITY RATIO = 2.9413
MEAN PEAK FACTOR (ON DISPLACEMENT) = 2.5280
AVERAGE MAXIMUM RELATIVE VELOCITY = 0.032690
AVERAGE MAXIMUM RELATIVE ACCELERATION = 0.105240
AVERAGE MAXIMUM ABSOLUTE ACCELERATION = 0.222960

RESULTS OF THE EQUIVALENT LINEAR ANALYSES

METHOD	PFC	PERIOD	DAMPING	DRC	RSVC	RSAC	ASAC
HEL	1.600	0.0689	0.23620	3.0251	0.039027	0.092911	0.241165
GSM	1.600	0.0664	0.22520	2.8133	0.037214	0.092092	0.240893
CCD	1.700	0.0677	0.18580	3.0319	0.041802	0.104092	0.247697

Table 17 Comparison of Response Prediction Using Various Methods

NATURAL FREQUENCY OF THE OSCILLATOR = 20.00
DAMPING RATIO FOR THE SYSTEM = 0.10
RATIO OF THE TWO SPRING STIFFNESSES = 0.25

RESPONSE FOR YIELD DISPLACEMENT = 0.0030

RESULTS OF TIME-HISTORY ANALYSIS

MEAN DUCTILITY RATIO = 4.2911
MEAN PEAK FACTOR (ON DISPLACEMENT) = 2.6170
AVERAGE MAXIMUM RELATIVE VELOCITY = 0.035190
AVERAGE MAXIMUM RELATIVE ACCELERATION = 0.103910
AVERAGE MAXIMUM ABSOLUTE ACCELERATION = 0.228480

RESULTS OF THE EQUIVALENT LINEAR ANALYSES

METHOD	PFC	PERIOD	DAMPING	DRC	RSVC	RSAC	ASAC
HEL	1.600	0.0758	0.25750	4.3890	0.044672	0.096894	0.243246
GSM	1.600	0.0712	0.24160	3.8909	0.041075	0.094699	0.242095
CCD	1.800	0.0733	0.19350	4.2968	0.047517	0.109543	0.250674

Table 18

General Guideline for Selection of Peak Factors

for Implementation of Various Models

Frequency Range	.25 - 2.50		2.50 - 9.00		9.0 - 35.0	
Method	1-4	4-10	1-4	4-10	1-4	4-10
HEL	2.0	1.7	1.6	-	1.7	1.6
GSM	2.0	1.7	1.6	-	1.7	1.7
CCD	2.0	2.2	1.9	2.2	1.9	2.2